Bifurcations Due to Nonlinear Reactivit Interactions in Lumped Parameter PHWR Dynamical Systems

by

K. MURALI

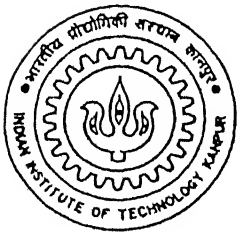

NUCLEAR ENGINEERING AND TECHNOLOGY PROGRAMME

INDIAN INSTITUTE OF TECHNOLOGY KANPUR

JULY 1998

Bifurcations Due to Nonlinear Reactivity Interactions in Lumped Parameter PHWR Dynamical Systems

A Thesis Submitted
in Partial Fulfilment of the Requirements
for the the Degree of

MASTER OF TECHNOLOGY

by

K. MURALI

to the

NUCLEAR ENGINEERING AND TECHNOLOGY PROGRAMME
INDIAN INSTITUTE OF TECHNOLOGY KANPUR
JULY 1998

Entered in System

Certificate

It is certified that work reported in the thesis entitled *Bifurcations due to Nonlinear Reactivity Interactions in Lumped Parameter PHWR Dynamical Systems*, by K. MURALI, has been carried out under my supervision and that this work has not been submitted elsewhere for a degree.

MSKalra

PROFFESSOR M. S. KALRA

Department of Mechanical engineering

and

Nuclear Engineering and Technology Programme

INDIAN INSTITUTE OF TECHNOLOGY KANPUR

July 1998

Acknowledgements

I would like to express my deep sense of gratitude to my guide Dr. M. S. Kalra for introducing me to the theory of bifurcation, for suggesting this problem, and patiently guiding me throughout this work.

I dutifully acknowledge the help and advice of Prof. Prabhat Munshi who acted as a friend and counsellor throughout my stay at IITK. My heartiest thanks to him.

I express my deep sense of gratitude to my parents for their love, affection and encouragements. I take this as an opportunity to express my love and affection to my brothers Santosh and Suresh. Their adorable patience and encouragement will remain with me forever.

My colleaques Surash Babu, Satyaprakash and Ram Manohar deserve special mention for their support and understanding which helped me in many ways. I strongly appreciate their willingness to help whenever asked for. Words are not sufficient to express my thankfulness to all my friends who made my stay at Hall-IV indeed memorable.

It is a pleasure to acknowledge the care and affection extended to me by the NET family members. My heartiest thanks to all of them.

ABSTRACT

Static and dynamic bifurcations due to nonlinear reactivity interactions in three-temperature lumped parameter PHWR dynamical systems are analysed. For the fuel and coolant temperature reactivity feedbacks, we consider both linear and higher-order (quadratic) feedback terms. For the moderator, while only linear feedback is considered, we allow both negative and slightly positive feedback coefficients. Models based on effective lifetime and prompt-jump approximations, as well as those based on one and six groups of delayed neutrons are considered. Besides the core and the moderator, two simple models of the steam generator, and proportionaland differential controllers are included in the analysis. The control signals may be based on fractional change in power and / or coolant temperature.

Data for analysis is derived from 220 Mwe and 500 Mwe PHWRs as well as from a number of other PHWRs in operation outside India. It is found that in all the reactors analysed, Hopf bifurcation occurs for negative values of coolant temperature coefficient of reactivity. Since the physical values of coolant temperature coefficient of reactivity is positive in PHWRs (under most operating conditions), the Hopf bifurcation is unlikely to occur. Even under those operating conditions where coolant temperature coefficient of reactivity may be negative, its magnitude is likely to be much smaller than that required for Hopf bifurcation, which is of the order of -10^{-2} K^{-1} in all the reactors considered. The static bifurcation in these reactors occurs for positive values of coolant temperature coefficient of reactivity of the order 10^{-3} to 10^{-4} K^{-1}, while the actual values is of the order 10^{-5} to 10^{-6} K^{-1}.

A worst- case analysis based on the most unfavourable combination of dimensionless parameters within certain specified ranges is also considered. In this case the values of coolant temperature coefficient of reactivity for which a static bifurcation is most likely to occur are found to be of the order of $+10^{-6}$ K^{-1}. While this value is physically realistic for PHWRs, it must be kept in mind that this applies when parameters of all reactors are combined in the worst manner.The worst-case parameters for Hopf bifurcation depend strongly on the moderator temperature coefficient of reactivity. The critical values of coolant temperature coefficient of reactivity, in particular, range from -4×10^{-5} to $+2 \times 10^{-4}$ K^{-1}.

Inclusion of control reactivity is shown to make bifurcations in the lumped parameter PHWR models further unlikely for all negative gains.

To My Parents

Contents

List of Figures

List of Tables

Nomenclature

A list of symbols is given below. Some symbols which are specific to a section, and whose meaning may be different in different sections, are not included. Standard mathematical symbols also do not appear in the list.

Roman

a_c	$\frac{\alpha_c(T_{co}-T_d)}{\beta}$, dimensionless
a_C	$\alpha_C(T_{co}-T_d)^2/\beta$, dimensionless
a_f	$\frac{\alpha_f(T_{fo}-T_d)}{\beta}$, dimensionless
a_F	$\alpha_F(T_{fo}-T_d)^2/\beta$, dimensionless
a_m	$\frac{\alpha_m(T_m-T_{mi})}{\beta}$, dimensionless
a_X	$\frac{\Gamma}{\upsilon\beta}\frac{\varphi_o-1}{\varphi_o}$, dimensionless
$a(0)$	normal form parameter $a(\varepsilon)$ at $\varepsilon = 0$
b	$\frac{\lambda\Lambda}{\beta}$, a nondimensionless parameter

b(0)	a normal form parameter $b(\varepsilon)$ at $\varepsilon = 0$
c	C_f / C_c
C_c	heat capacity of coolant in reactor core, JK^{-1}
C_f	heat capacity of fuel elements in core. JK^{-1}
C_m	heat capacity of the moderator in the calandria, JK^{-1}
C_s	effective heat capacity of the secondary side, JK^{-1}
$\subset$	$(C-C_o) / C_o$
$I, I(t)$	average concentration of iodine-135 m^{-3}
I	$\frac{I - I_o}{I_o}$
N, N(t)	number of neutrons
p	$\frac{\Lambda P_0}{\beta C_f (T_{f0} - T_{c0})}$
P, P(t)	reactor power, W
$\wp$	$\frac{P - P_o}{P_o} = \frac{N - N_o}{N_o}$
q	$\frac{\delta P \Lambda_o}{C_m \beta (T_{mo} - T_{mc})}$
r	$\frac{\Lambda P_o}{C_s \beta (T_{co} - T_{so})}$
t	time, s
T	time-period or characteristic time (in specified units or dimensionless)
$T_c, T_c(t)$	average coolant temperature, K

T_f, $T_f(t)$ average fuel temperature, K

T_m, $T_m(t)$ average coolant temperature, K

$\Im_c$ $\dfrac{T_c - T_{co}}{T_{co} - T_i}$

$\Im_f$ $\dfrac{T_f - T_{fo}}{T_{fo} - T_i}$

$\Im_s$ $\dfrac{T_s - T_{so}}{T_{co} - T_{so}}$

$\Im_m$ $\dfrac{T_m - T_{mo}}{T_{mo} - T_{mi}}$

U, U(η) Jacobian matrix of the vector field at **X**=0

V (X,η) vector field

W(X,η) nonlinear part of the vector field

χ $\dfrac{X - X_o}{X_o}$

X, X(τ) state vector at time τ

Greek

α_c coolant temperature coefficient of reactivity, K^{-1}

α_f fuel temperature coefficient of reactivity, K^{-1}

α_m moderator temperature coefficient of reactivity, K^{-1}

α_C second order coolant temperature coefficient of reactivity, K^{-2}

α_F second order fuel temperature coefficient of reactivity, K^{-2}

β one group delayed neutron fraction

η a set of dimensionless parameters

λ one-group decay constant for delayed neutron precursors, s^{-1}

Λ neutron reproduction or generation time, s

θ $\dfrac{T_{co} - T_d}{T_{fo} - T_d}$

ρ reactivity, dimensionless

ρ_{fb} feedback reactivity

ρ_c control reactivity

ρ_X reactivity feedback due to xenon-135

τ $\beta t / \Lambda$, dimensionless time

ϕ flux of thermal neutrons, $m^{-2}\ s^{-1}$

φ_o $1 + \dfrac{\sigma_X \phi_o}{\lambda_X}$, dimensionless

$\Phi, \Phi(t)$ fundamental or state transition matrix

Miscellaneous

\$ ρ / β

Subscripts

R a reference value

o a steady state value

Superscripts

* a critical value

Chapter 1

Introduction

1.1 Motivation

Nonlinear time evolution and stability of a dynamical system, e.g., an engineering or a physical system described by a set of coupled nonlinear ordinary differential equations (ODEs) are intimately related to the local bifurcation phenomena that arise in the steady-state form of ODEs. Every problem in applications in general contains several physical parameters which may vary over certain specified sets. Thus it is important to understand the qualitative behavior of the system as the parameters vary. A good design for a system will always be such that the qualitative behavior does not change when the parameters are varied a small amount about the value for which the original system was made. However, the behavior may change when the system is subjected to large variations in the parameters. A change in the qualitative properties could mean a change in the stability of the original system and thus the system must assume a state different from the original design. The values of the parameters where this change takes place are called bifurcation values. Knowledge of bifurcation values is absolutely necessary for a complete understanding of the system.

The concepts of bifurcation theory, stability theory and nonlinear dynamics are also applicable to the dynamics of nuclear systems and can provide crucial information for the safe operation of nuclear reactors. The dynamic models of nuclear systems are nonlinear even with linear feedback effects. Nonlinearities in the reactor dynamical systems arise due to strong interactions between neutronics, thermal-hydraulics and fission product poisoning. The nonlinear model is normally linearised around steady state operating point at full power leading to the representation of the system by a set of linear ordinary differential equations. These equations are transformed into state space form to yield a linear time invariant system for the reactor, which is then studied using classical methods applicable to the linear systems. At present time, it appears that the techniques of nonlinear systems research have not been as fully and widely utilized in the nuclear energy field as in the other branches of scientific knowledge. This work applies some of these techniques to lumped parameter PHWR dynamical systems.

1.2 Objectives

The overall objective of the present work is to study several fission reactor dynamical systems, representative of lumped parameter PHWRs in a comparative manner, with a view to understand the role of intrinsic reactor core nonlinearities arising due to thermal-hydraulic and fission product reactivity feedbacks. For this purpose, we choose phenomenological models with varying degrees of approximation for the core, moderator, steam generator and the control system. The emphasis will be on the local bifurcation phenomena near steady state operating point. Both the static and dynamic bifurcations are studied and the parameter ranges over which bifurcations occur are identified.

1.3 Review of Literature

An extensive review of the literature related to the bifurcation studies applied to PWRs and BWRs has been presented by Kalra and Sriram (1998); Manmohan (1996). A brief review of these studies applicable to PHWRs is given here. The mathematical and physical importance of the nonlinear form of reactor kinetics equations, when the effect of temperature is included, was pointed out by Chernick (1951). Robinson (1954, 1955) extended the treatment of Chernick (1951) in regard to concept of reactor stability and included the effect of delayed neutrons. The concepts of orbital, secular and asymptotic stability are examined in the phase plane representation and techniques are pointed out whereby the effect of the delayed neutrons on reactor kinetics may be taken into consideration. Hsu (1968), Kastenberg (1968), and Hsu and Sha (1969) considered the stability problem for spatially dependent nonlinear reactor systems and pointed out that in a practical reactor the delayed neutrons must be included and more than one feedback should be considered. Enginol (1985) has analyzed asymptotic stability of nuclear reactors with arbitrary nonlinear feedback. Ward and Lee (1987a, 1987b) have used a singular perturbation method for the analysis of large amplitude power oscillations in nuclear reactors. Adebiyi and Harms(1989, 1990) examine some aspects of linear and nonlinear nuclear reactor kinetics by general topological methods. Bergdahl, *et al.* (1989) analyze the stability and other safety-related problems at Forsmark-1 and point out that the instability is caused by the dynamic coupling between the neutron kinetics and thermal-hydraulics *via* void reactivity feedback. Dorning(1989) provides a general discussion of strange atrractors in the context of nuclear reactors. Hopf bifurcation in the context of xenon oscillations is discussed by Rizwan-uddin (1989). Yang and cho (1992) present expansion methods for finding nonlinear stability domains of nuclear reactor models.

The data of different PHWRs used in this work is based on the data given in Power Reactors (1983) and World Nuclear Industry Handbook (1994). Data of the typical features of standard 220 MWe and 500 MWe Pressurized Heavy Water Reactors (PHWRs) with natural uranium as fuel are given in AERB (1997); Bagchi (1994); NPCIL (1992). A three-temperature model has

been developed for PHWRs taking moderator feedback into consideration based on the discussions presented by BARC (1987); Rastogi (1976); BHEL. Lewins (1978) presented detailed analysis of classical control methods applied to linear reactor dynamical systems. He also developed a suitable lumped parameter model for the boiler / steam generator, which has been adapted for the present work.

1.4 Outline of the Present Work

Later in this chapter in Sections 1.5 and 1.6 , a brief description of PHWRs and reactivity effects of temperature is presented. In Chapter 2 , lumped parameter models for core, moderator, steam generator and control system based on linear reactivity feedback using delayed neutrons represented by one or six groups have been formulated. Aspects of higher-order reactivity feedback essential for Static bifurcation analysis are included. Simplications based on effective lifetime and prompt-jump approximations are also presented, together with the conditions for their validity. All the governing equations are presented in a dimensionless form, and incorporate an appropriate translation of the state variables required for later analysis.

In Chapter 3, the phenomena of Hopf bifurcation and static bifurcation (transcritical) bifurcation in the fission reactor dynamical systems are investigated. The numerical scheme for locating the bifurcation points in different models is discussed , followed by the calculation of center manifold at Hopf and static bifurcations. The effect of system parameters on the critical value and the stability parameter is also examined.

Numerical results on the behavior of the dynamical systems at the close vicinity of bifurcation points are presented in Chapter 4. A summary of the work done and conclusions reached, together with a few observations on the possible extension of the present work are also presented.

1.5 A Brief Description of PHWR

A Pressurized Heavy Water Reactor (PHWR) is a horizontal pressure tube type reactor using natural uranium dioxide fuel with heavy water moderator and high pressure heavy water coolant (BARC, 1987; Rastogi, 1976). The fuel and the moderator are contained in a horizontal cylindrical shell and tube assembly known as calandria. Cold pressed and sintered pellets of uranium dioxide (UO_2) in zircaloy tubes form the cylindrical fuel elements. The shell of the calandria contains heavy water moderator.

The moderator and the coolant have their own closed circulating systems. The coolant system. called the Primary Heat Transport (PHT) system, is a high pressure and high temperature circuit with no bulk boiling. The moderator circuit is at low pressure and low temperature. These two are insulated from each other in the reactor core by a gas annulus between the calandria and the coolant tubes. The actual data for different PHWRs studied in the present work is given later in Chapter 2. A schematic diagram of a PHWR is given in Figure 1.

1.6 Temperature Effects On Reactivity

The reactor operation at power causes changes in the temperature of fuel, coolant and the moderator. These changes in temperature cause changes in reactivity which in turn affect the power. This change in power again changes the temperatures. Thus a feedback process is established. Therefore, variation of reactivity with temperature of the fuel, coolant and moderator is an important factor in the reactivity control and the safety of the power reactor.

The rate of change of reactivity with respect to temperature is defined as the temperature coefficient of reactivity, and is expressed as K^{-1}. The effect of the fuel temperature on the reactivity is the main contributing factor to power coefficient. The latter with coolant temperature coefficient is important for safety assessment during a rapid power transient. The reactivity

variation with coolant temperature is important in the assessment of safety aspects associated with faults in the coolant system. The usefulness of the moderator temperature coefficient lies in its potential applicability to fine reactivity control. The three temperature coefficients of reactivity used in the present work are described below.

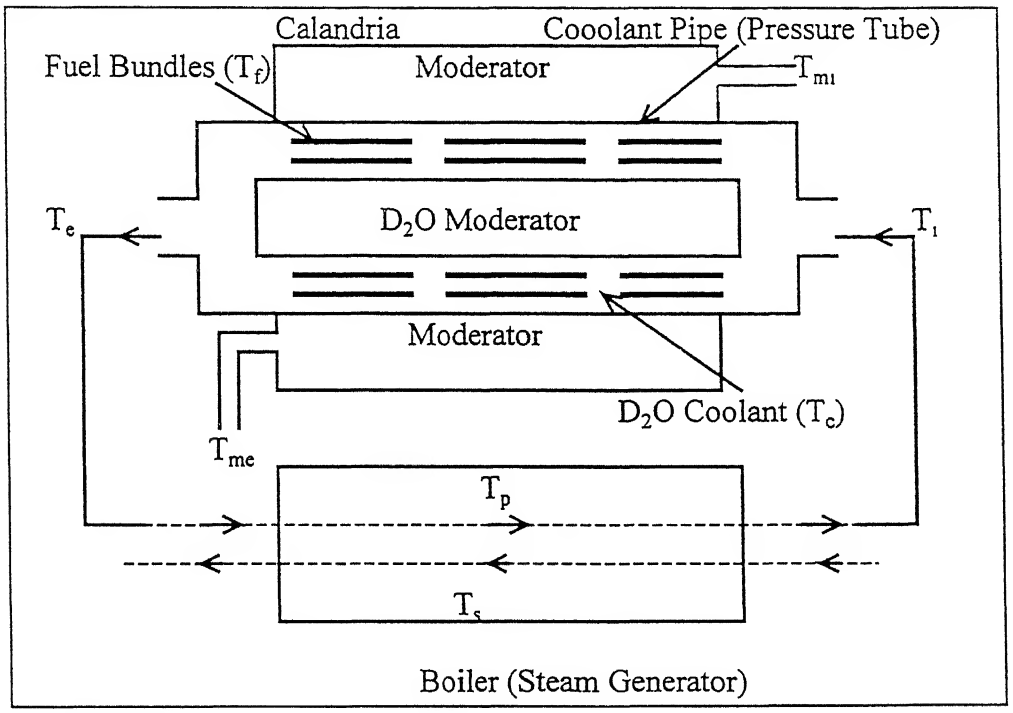

Figure 1: A schematic diagram of a PHWR system with Steam Generator (SG)

Fuel Temperature Coefficient

There are two factors which significantly affect the fuel temperature coefficient:

(1) Doppler Effect

When fuel temperature increases, the thermal motion of fuel atoms also increases and the energy range over which resonance capture occurs is broadened resulting in increased resonance absorption. This is called Doppler effect. Hence an increase in fuel temperature causes an increase in the absorption cross-section of fuel, particularly of U^{238}.

(2) Neutron Temperature Effect

The physical temperature of the fuel affects the fuel neutron temperature because of some speeding-up of neutrons in the hot fuel. Due to increase in the temperature of the fuel, the average energy of the neutron increases and the spectrum is shifted towards higher energy.

Coolant Temperature Coefficient

The effect of coolant temperature on reactivity arises from the changes that occur in the density of the coolant and in the neutron speeding-up effect in the fuel as a result of the change in coolant temperature, i.e., due to neutron temperature effect. With increase in coolant temperature, the density of the coolant decreases, which causes macroscopic absorption crosssections to decrease and mean free paths to increase. This in turn affects the reactivity.

Moderator Temperature Coefficient

The variation of reactivity with moderator temperature arises from two effects:

(1) The density change, associated with the change in moderator temperature, affects the moderating properties of heavy water.

(2) An increase in moderator temperature also causes the thermal neutron spectrum to be shifted towards slightly higher energy range at which the cross-sections are different.

Chapter 2

Lumped Parameter PHWR Dynamical Systems

2.1 Neutron Kinetics

The point-reactor kinetics equations with one group of delayed neutrons can be written as (Lewins 1978, Hetrick 1971) :

$$\frac{dN}{dt} = \frac{\rho-\beta}{\Lambda} N + \lambda C \text{ , and} \qquad (2.1)$$

$$\frac{dC}{dt} = \frac{\beta}{\Lambda} N + \lambda C \text{ ,} \qquad (2.2)$$

where

N = $N(t)$ is the number of neutrons or average neutron density in the reactor,

C = C(t) is the number of delayed neutron precursors or average delayed neutron precursor density,

t = time(s),

Λ = neutron reproduction or generation time (s),

β = delayed neutron fraction (dimensionless),

λ = decay constant for delayed neutron precursors (s^{-1}),

ρ = reactivity or fractional excess multiplication constant (dimensionless).

2.2 Power Balances

The three-temperature feedback model is based on three power balances: one for the energy contained in the fuel elements of the reactor core, second for the energy stored in the coolant within the core volume, and another for the fission energy deposited directly in the moderator.

The power balance for the *fuel elements* is given by

$$C_f \frac{dT_f}{dt} = P - H_f(T_f - T_c) \qquad (2.3)$$

where

T_f = $T_f(t)$ is the average fuel temperature (K),

T_c = $T_c(t) = \frac{T_i + T_e}{2}$ is the mean coolant temperature (K),

T_i = coolant inlet temperature (K),

T_e = coolant exit temperature (K),

P = $P(t)$ is the reactor power (W),

C_f = heat capacity of fuel elements in the reactor core (JK^{-1}),

and

H_f = fuel to coolant heat transfer constant (WK^{-1}).

The power balance for the *coolant* in the reactor core is given by

$$C_c \frac{dT_c}{dt} = H_f(T_f - T_c) - 2\dot{m}_c c_c(T_c - T_i) \qquad (2.4)$$

where

C_c = heat capacity of the coolant in the reactor core (JK^{-1}),

m_c = mass flow rate of coolant through the core (kgs^{-1}),

c_c = specific heat of the coolant ($J\ kg^{-1}K^{-1}$).

The power balance for the *moderator* is given by

$$C_m \frac{dT_m}{dt} = \delta\ P - 2 m_m\, c_m (T_m - T_{mi}) \qquad (2.5)$$

Two types of power balance for the moderator have been considered in the present work:

(1) Constant heat removal rate

In this model the quantity $2 m_m\, c_m (T_m - T_{mi})$ is a constant and is equal to $\delta\ P_o$. Hence Eq. 2.5 becomes

$$C_m \frac{dT_m}{dt} = \delta P - \delta P_o = \delta (P - P_o) \qquad (2.6)$$

(2) Heat removal rate proportional to moderator temperature

In this model Eq. 2.5 represents the power balance for the moderator with the moderator temperature T_m appearing on both sides of the equation.

The symbols in Eqs. 2.5 and 2.6 are as follows :

C_m = heat capacity of the moderator in the calandria (JK^{-1}) ,

δ = fraction of fission energy deposited directly in the moderator,

$\dot{m}_m$ = flow rate of the moderator through the calandria (kgs^{-1}),

c_m = specific heat of the moderator (J $kg^{-1}K^{-1}$),

T_m = $T_m(t) = \frac{T_{me} + T_{mi}}{2}$ is the mean moderator temperature (K),

T_{mi} = inlet moderator temperature to the calandria (K),

T_{me} = exit moderator temperature from the calandria (K), and

P_o = steady state power (W).

The power balance for the *boiler / Steam Generator* (SG) is given by

$$C_s \frac{dT_s}{dt} = H_s(T_c - T_s) - m_s \Delta h \qquad (2.7)$$

Two types of power balance for the SG have been derived in the present work :

(1) Constant secondary side temperature

In this model the quantity $\frac{dT_s}{dt} = 0$ and hence RHS of the Eq. 2.7 becomes

$$m_s \Delta h = H_s(T_c - T_s) = 2 m_c c_c (T_c - T_i) \qquad (2.8)$$

The second equality in the above equation is based on the assumption that no heat loss takes place in the coolant pipes which transport the primary coolant from the reactor to the SG.

(2) Constant power removal from the secondary side

In this model the second term on the RHS of Eq. 2.7 is considered constant, i.e.,

$$\dot{m}_s \Delta h = P_o$$

In this case the power balance of SG is given by

$$C_s \frac{dT_s}{dt} = H_s(T_c - T_s) - P_o \qquad (2.9)$$

In Eqs. 2.7 to 2.9, the symbols are as follows :

C_s = effective heat capacity of the secondary side (JK^{-1})

m_s = steam production rate on the secondary side (kgs^{-1}),

Δh = specific enthalpy change on the secondary side (Jkg^{-1}),

H_s = primary to secondary side heat transfer constant (WK^{-1}),

T_s = $T_s(t)$ is saturation temperature corresponding to the secondary side.

2.3 Steady State Relations

The steady state operating values of the state variables in Eqs. 2.1-2.9 will be denoted by $P_o, C_o, T_{fo}, T_{co}, T_{mo}, T_{so}$ respectively, and the steady state value of the reactivity is taken as ρ_o. By equating Eqs. 2.1-2.5 and 2.9 to zero, we obtain

$$\rho_o = 0, \qquad C_o = \frac{\beta}{\Lambda} P_o$$

$$H_f = \frac{P_o}{T_{fo} - T_{co}}, \qquad 2 m_c c_c = \frac{P_o}{T_{co} - T_{io}}, \qquad (2.10)$$

$$2 m_m c_m = \frac{\delta}{T_{mo} - T_{mi}} P_o \text{ , and } H_s = \frac{\dot{m}_s \Delta h}{T_{co} - T_{so}} \equiv \frac{P_o}{T_{co} - T_{so}},$$

where T_{io} is the steady state value of T_i, the coolant inlet temperature to the reactor. In models without the steam generator, T_i is considered a constant.

2.4 Linear Reactivity feedback

The reactivity ρ appearing in Eq. 2.1 can, in general, be written as

$$\rho = \rho_o + \rho_e(t) + \rho_c + \rho_{fb} .$$

As seen above, if there is no external source of neutrons in the reactor, as is the case considered throughout the present work, $\rho_o = 0$. For the autonomous system we treat $\rho_e(t) = 0$. The control reactivity ρ_c is considered separately in Section 2.10. Further, the dynamical systems developed in this chapter are based on linear reactivity feedback which for the three temperature PHWR model can be written as

$$\rho = \rho_{fb} = \alpha_f (T_f - T_{fo}) + \alpha_c (T_c - T_{co}) + \alpha_m (T_m - T_{mo}) \qquad (2.11)$$

where

α_f = Doppler or fuel temperature coefficient of reactivity (K^{-1}),

α_c = coolant-moderator temperature coefficient of reactivity (K^{-1}), and

α_m = moderator temperature coefficient of reactivity (K^{-1}).

Reactivity effects of xenon and Higher-order feedback are considered in Section 2.7 and 2.9.

It is the substitution of Eq. 2.11 in Eq. 2.1 which is one source of nonlinearity in the fission reactor dynamical systems. It leads to product terms of $P(t), T_f(t), T_c(t)$ and $T_m(t)$. Instead of presenting the resulting equations, we first choose suitable non-dimensional forms of dependent state variables and the independent time variable.

2.5 Dimensionless Equations

In order to obtain the previous equations in a dimensionless form we choose the following translation and scaling of the state variables and time:

$$\wp = \frac{P - P_o}{P_o} \equiv \frac{N - N_o}{N_o}, \qquad \subset = \frac{C - C_o}{C_o},$$

$$\Im_f = \frac{T_f - T_{fo}}{T_{fo} - T_d}, \qquad \Im_c = \frac{T_c - T_{co}}{T_{co} - T_d}, \qquad (2.12)$$

$$\Im_s = \frac{T_s - T_{so}}{T_{co} - T_{so}}, \qquad \text{and} \qquad \Im_m = \frac{T_m - T_{mo}}{T_{mo} - T_{mi}}$$

$$\tau = \frac{\beta}{\Lambda} t.$$

where

$T_d = T_i = T_{io}$ if the SG models are not included in the dynamical systems and

$= T_{so}$ if the SG models are included in the dynamical systems.

The translations of the state variables in the above equations shift the operating or equilibrium point to the origin. This is essential for the analysis presented in later chapters. The normalizations used could be chosen differently, but the above choice puts the dynamical system in the simplest form. Substitution of Eqs. 2.11 and 2.12 into Eqs. 2.1-2.9 and using Eqs. 2.10 where needed leads to the following dimensionless system:

$$\frac{d\wp}{d\tau} = -\wp + \subset + a_f T_f + a_c T_c + a_m T_m + a_f \wp T_f + a_c \wp T_c + a_m \wp T_m, \qquad (2.13)$$

$$\frac{d\subset}{d\tau} = b(\wp - \subset), \qquad (2.14)$$

$$\frac{d\Im_f}{d\tau} = p(1-\theta)\wp - p\Im_f + p\theta\Im_c, \qquad (2.15)$$

If the secondary side temperature on the SG is constant then we have for the dimensionless equation of coolant (model 1, Eq. 2.8) as

$$\frac{d\Im_c}{d\tau} = \frac{pc}{\theta}(\Im_f - \Im_c), \qquad (2.16)$$

On the other hand, if power removal in the SG is constant (model 2, Eq. 2.9) then the dimensionless equation for the coolant is given by

$$\frac{d\Im_c}{d\tau} = \frac{pc}{\theta}(\Im_f - \Im_c + (1-\theta)\Im_s) \qquad (2.17)$$

For the moderator model 1 (Eq. 2.6), the dimensionless form of the moderator is given by

$$\frac{d\Im_m}{d\tau} = q\,\wp \tag{2.18}$$

For the moderator model 2 (Eq. 2.8), the dimensionless equation for the moderator is given by

$$\frac{d\Im_m}{d\tau} = q(\wp - \Im_m). \tag{2.19}$$

This completes the dynamical system if steam generator is excluded or model 1 is taken for the SG. However, if model 2 of the SG is taken, the above equations are supplemented by the following equation governing the dimensionless secondary side temperature:

$$\frac{d\Im_s}{d\tau} = r(\Im_c - \Im_s) \tag{2.20}$$

In Eqs. 2.13 to 2.20, the nondimensional parameters are as follows :

$$a_f = \frac{\alpha_f (T_{fo} - T_d)}{\beta}, \qquad a_c = \frac{\alpha_c (T_{co} - T_d)}{\beta},$$

$$a_m = \frac{\alpha_m (T_m - T_{mi})}{\beta} \qquad b = \frac{\lambda}{\beta}\Lambda$$

$$p = \frac{\Lambda P_o}{\beta C f (T_{fo} - T_{co})}, \qquad \theta = \frac{T_{co} - T_d}{T_{fo} - T_d} \tag{2.21}$$

$$c = \frac{C_f}{C_c} \qquad q = \frac{\delta P \Lambda_o}{C_m \beta (T_{mo} - T_{mc})}$$

$$r = \frac{\Lambda P_o}{C_s \beta (T_{co} - T_{so})}$$

where as mentioned earlier, $T_d = T_{10}$ if the steam generator is excluded from the dynamical system, and $T_d = T_{so}$ otherwise.

It can be seen that the original system of the three-temperature linear feedback model has been transformed to a dimensionless system with the nine non-dimensional parameters. The parameters a_f, a_c and a_m can be interpreted as the dimensionless measures of temperature coefficients of reactivity. The parameter p may understood to measure the steady state power P_o of the reactor, the other terms in the expression being relatively fixed or showing lesser variation for a given reactor. The parameters b, θ, c, q, and r are viewed as simple dimensionless combinations of input quantities.

Considering model 2 of the moderator and the SG (for illustration), the above dimensionless equations can be written in the form of a state equation :

$$\dot{\mathbf{X}} = \mathbf{V}(\mathbf{X},\eta)$$

$$= \mathbf{U}(\eta)\mathbf{X} + \mathbf{W}(\mathbf{X},\eta) \qquad (2.22)$$

where the overdot denotes the derivative with respect to dimensionless time τ, $\mathbf{X}$ is the state vector , η is the set of dimensionless parameters (Eqs 2.21), and $V(X,\eta)$ is the vector field whose linear part is $U(\eta)X$ and the nonlinear part is $W(X,\eta)$, i.e.,

$$\mathbf{X} = \begin{bmatrix} X_1 \\ X_2 \\ X_3 \\ X_4 \\ X_5 \\ X_6 \end{bmatrix} = \begin{bmatrix} \wp \\ \subset \\ \Im_f \\ \Im_c \\ \Im_m \\ \Im_s \end{bmatrix}, \qquad \mathbf{W}(\mathbf{X},\eta) = \begin{bmatrix} a_f X_1 X_3 + a_c X_1 X_4 + a_m X_1 X_5 \\ 0 \\ 0 \\ 0 \\ 0 \\ 0 \end{bmatrix}$$

$$\mathbf{U}(\eta) = \mathbf{D}_X \mathbf{V}(\mathbf{X}_o, \eta) = \begin{bmatrix} -1 & 1 & a_f & a_c & a_m & 0 \\ b & -b & 0 & 0 & 0 & 0 \\ p(1-\theta) & 0 & -p & p\theta & 0 & 0 \\ 0 & 0 & \frac{pc}{\theta} & -\frac{pc}{\theta} & 0 & \frac{pc}{\theta}(1-\theta) \\ q & 0 & 0 & 0 & -q & 0 \\ 0 & 0 & 0 & r & 0 & -r \end{bmatrix}$$

and

$$\eta = \{a_f, a_c, a_m, b, p, \theta, c, q, r\},$$

where $\mathbf{X}_o = 0$ is a solution of $\mathbf{V}(\mathbf{X},\eta) = 0$ for all η. It is clear that

$$\mathbf{W}(0,\eta) = 0 \text{ and } \mathbf{D}_X \mathbf{W}(0,\eta) = 0.$$

2.6 Six Groups of Delayed Neutron Precursors

Six groups appear to be the optimum for an accurate representation of delayed neutron precursors. For the calculation of the critical value of a parameter at which a bifurcation may take place, it is therefore desirable to use six groups of delayed neutron emitters. This is achieved by replacing Eq. 2.14 by six differential equations governing the populations of different delayed neutron precursors.

$$\frac{d\subset_i}{d\tau} = b_i(\wp - \subset_i), \qquad i = 1.,.....,6, \qquad (2.23)$$

where

$$\subset_i = \frac{C_i - C_{io}}{C_{io}},$$

C_i = population of the precursor group i,

C_{io} = steady state population of the precursor group i,

$$b_i = \frac{\lambda_i \Lambda}{\beta},$$

$$\beta = \sum_{i=1}^{6} \beta_i,$$

β_i = delayed neutron fraction for the i^{th} precursor group,

λ_i = decay constant of the i^{th} precursor group (s^{-1}),

and other variables or constants are as defined earlier in this chapter. Simultaneously, the term $\subset$ in Eqs. 2.13 is replaced by:

$$\subset = \sum_{i=1}^{6} a_i \subset_i,$$

where $a_i = \frac{\beta_i}{\beta}$ is the relative yield for the precursor group i. For the purpose of parameter variations in the six group models, instead of treating each b_i as a variable parameter, we write

$$b_i = \left(\frac{\lambda_i}{\lambda}\right) b, \qquad \text{and} \qquad \lambda = \frac{1}{\sum_{i=1}^{6} \frac{a_i}{\lambda_i}},$$

where b has been previously defined (Eqs. 2.21) and is treated as a possibly variable parameter as in one group models.

2.7 Reactor Models with Xenon Poisoning

Fission-product poisoning plays a vital role in the operation of power-producing thermal reactors. Because of their large thermal-neutron absorption cross sections, two nuclides are of particular interest, xenon-135 and samarium-149. Since samarium-149 has a somewhat lower cross section for thermal neutrons , it does not contribute as much to the poisoning of a reactor as does the xenon 135 and hence it is neglected.

Denoting by I and X the time-dependent concentrations of I^{135} and Xe^{135} respectively, we have (Lewins, 1978):

$$\frac{dI}{dt} = \gamma_I \Sigma_f \phi - \lambda_I I, \text{ and} \tag{2.24}$$

$$\frac{dX}{dt} = \gamma_X \Sigma_f \phi + \lambda_I I - \lambda_X X - \phi \sigma_X X, \tag{2.25}$$

where

γ_I = yield of iodine atoms per fission,

γ_X = yield of xenon atoms per fission,

λ_I = decay constant for iodine, s^{-1},

λ_X = decay constant for xenon, s^{-1},

σ_X = microscopic absorption cross section of xenon for thermal neutrons, m^2,

Σ_f = macroscopic fission cross section, m^{-1}, and

ϕ = flux of thermal neutrons, $m^{-2} s^{-1}$.

As in the previous sections of this chapter, in order to put Eqs. 2.24 and 2.25 in a dimensionless form, we begin by defining

$$\mathrm{I} = \frac{I - I_o}{I_o}, \qquad \text{and} \qquad \chi = \frac{X - X_o}{X_o}, \tag{2.26}$$

where I_o and X_o are the steady state concentrations of iodine and xenon obtained by equating the right-hand sides of Eqs. 2.24 and 2.25 to zero:

$$I_o = \frac{\gamma_I \Sigma_{f_o} \phi_o}{\lambda_I}, \quad \text{and} \quad X_o = \frac{\Gamma \Sigma_{f_o} \phi_o}{\lambda_X + \phi_o \sigma_X}, \tag{2.27}$$

where $\Gamma = \gamma_I + \gamma_X$ and ϕ_o is the steady state value of thermal neutron flux.

Introducing Eqs. 2.26 into Eqs. 2.24 and 2.25 using (in the context of a point reactor model)

$$\frac{\phi - \phi_o}{\phi_o} = \frac{P - P_o}{P_o} = \wp,$$

we obtain the following dimensionless equations:

$$\frac{d\mathrm{I}}{d\tau} = \zeta(\wp - \mathrm{I}), \quad \text{and} \tag{2.28}$$

$$\frac{d\chi}{d\tau} = \xi(1 - \gamma\varphi_o)\wp + \xi\gamma\varphi_o \mathrm{I} - \xi\varphi_o\chi - \xi(\varphi_o - 1)\wp\chi, \tag{2.29}$$

where τ is the dimensionless time as defined earlier, and

$$\zeta = \frac{\lambda_I \Lambda}{\beta}, \qquad \xi = \frac{\lambda_X \Lambda}{\beta},$$

$$\varphi_o = 1 + \frac{\sigma_X \phi_o}{\lambda_X}, \quad \text{and} \quad \gamma = \frac{\gamma_I}{\Gamma} \tag{2.30}$$

are the four dimensionless parameters governing the behavior of xenon and iodine.

The last term in Eq. 2.29 represents the nonlinearity in the governing equation for xenon. In order to consider the effect of xenon poisoning on any of the dynamical systems presented earlier, the following procedure is adopted:

(i) Append Eqs 2.28 and 2.29 to the dynamic model under consideration.

(ii) Include the reactivity effect due to xenon on the right hand side of the reactivity feedback Eqs. 2.11.

The reactivity feedback due to xenon is given by

$$\rho_X = -\frac{\sigma_X (X - X_o)}{\upsilon \Sigma_f} \quad , \tag{2.31}$$

where υ is the average number of neutrons produced per fission and the other variables are as defined earlier. The constants appearing in Eq. 2.31 can be replaced in terms of the dimensionless variables defined previously. This yields:

$$\$_X = a_X \chi , \tag{2.32}$$

where

$$a_X = -\frac{\Gamma}{\upsilon\beta}\frac{\varphi_o - 1}{\varphi_o}, \tag{2.33}$$

and χ is given by Eq. 2.26 . This reactivity as other feedback reactivities due to (three) temperature and effects, interacts parametrically with neutron population when introduced in Eq. 2.1 yielding an additional linear and nonlinear term in the equation governing neutron population. It is straight forward to see that if the resulting equations are collected in the form of the state equation (Eq. 2.22), we have the following variants of the dynamical system (with one group of delayed neutrons with models 2 of moderator and SG) :

PHWR Model with Xenon

$$X = \begin{bmatrix} X_1 \\ X_2 \\ X_3 \\ X_4 \\ X_5 \\ X_6 \\ X_7 \\ X_8 \end{bmatrix} = \begin{bmatrix} \wp \\ \subset \\ \Im_f \\ \Im_c \\ \Im_m \\ \Im_s \\ \mathrm{I} \\ \aleph \end{bmatrix}, \qquad W(X,\eta) = \begin{bmatrix} a_f X_1 X_3 + a_c X_1 X_4 + a_m X_1 X_5 + a_X X_1 X_8 \\ 0 \\ 0 \\ 0 \\ 0 \\ 0 \\ 0 \\ -\xi(\varphi_o - 1) X_1 X_8 \end{bmatrix}$$

$$U(\eta) = \begin{bmatrix} -1 & 1 & a_f & a_c & a_m & 0 & 0 & a_X \\ b & -b & 0 & 0 & 0 & 0 & 0 & 0 \\ p(1-\theta) & 0 & -p & p\theta & 0 & 0 & 0 & 0 \\ 0 & 0 & \frac{pc}{\theta} & -\frac{pc}{\theta} & 0 & \frac{pc}{\theta}(1-\theta) & 0 & 0 \\ q & 0 & 0 & 0 & -q & 0 & 0 & 0 \\ 0 & 0 & 0 & r & 0 & -r & 0 & 0 \\ \varsigma & 0 & 0 & 0 & 0 & 0 & -\varsigma & 0 \\ \xi(1-\gamma\varphi_o) & 0 & 0 & 0 & 0 & 0 & \xi\gamma\varphi_o & -\xi\varphi_o \end{bmatrix}$$

and

$$\eta = \left\{ a_f, a_c, a_m, a_X, b, p, c, \theta, q, r, \varphi_0 \right\}$$

is the new set of parameters. Here the dimensionless quantities ζ, ξ, Γ and γ are treated as basic physical constants and not as variable parameters. The quantities υ and β which appear in the expression for a_X are also considered relatively fixed. This leaves φ_o as the only new nondimensional parameter which may varied due to operation at different steady state neutron flux ϕ_o.

2.8 Simpler Dynamical Models

In the dynamical models presented in the previous sections, the delayed neutrons have been treated using one or six precursor groups. One group is convenient and often satisfactory. Further simplification is afforded by the effective lifetime model and the prompt-jump approximations. In the following subsections these models are briefly described and the governing equations are presented in the dimensionless form used in the present work.

Effective Lifetime Model

The effective lifetime Λ' of neutrons may be defined as (Hetrick, 1971; Lewins, 1978):

$$\Lambda' = \Lambda + \frac{\beta}{\lambda} \approx \frac{\beta}{\lambda} \qquad (2.34)$$

If, in the preceding equations, Λ is replaced by Λ', and the state variable as well as the equation(s) corresponding to the delayed neutron precursors are dropped, we obtain the lumped parameter dynamic equations based on the effective lifetime of neutrons. This model is sometimes easier to analyze but is applicable only when the reactivity and the rate of change reactivity are small :

$$\frac{1}{\lambda}\left|\frac{d\rho}{dt}\right| << |\rho| << \beta, \qquad (2.35)$$

or, in terms of the dimensionless variables used in this work,

$$|\$| << 1, \text{ and } \left|\frac{d\$}{d\tau}\right| << b|\$| \qquad (2.36)$$

where \$ = $\frac{\rho}{\beta}$ and b is defined earlier in this chapter.

Prompt-Jump Approximation

The prompt-jump approximation or , as it is sometimes called, the zero-lifetime approximation, described in detail by Hetrick (1971). Formally, an expansion of the neutron population or density in powers of the small parameter Λ is attempted, the procedure being analogous to the method of singular perturbations. If this approximation is used, the point-reactor kinetics Eqs. 2.1 and 2.2 are replaced by the following single equation :

$$\frac{dN}{dt} \approx \frac{\lambda\rho + \frac{d\rho}{dt}}{\beta - \rho} N \qquad (2.37)$$

In Eq. 2.37 the reactivity ρ must be substituted through Eq. 2.11, in terms of the other variables. This makes the Eq. 2.37 for the neutron population nonlinear, as is the case in other models. The criterion for the validity of prompt-jump approximation is (Hetrick, 1971):

$$\frac{1}{N}\left|\frac{dN}{dt}\right| << \frac{\beta - \rho}{\Lambda} \qquad (2.38)$$

It should be noted that the criterion (2.38) can only be satisfied if $\rho < \beta$, i.e., \$ < 1. In terms of the dimensionless variables defined earlier, the prompt-jump approximation can be written as

$$\wp \approx \frac{(1+\wp)(\$ + b\$)}{(1-\$)}, \qquad (2.39)$$

which is applicable if the following condition, equivalent to (2.38), is satisfied:

$$\frac{|\wp|}{(1+\wp)(1-\$)} << 1. \qquad (2.40)$$

where the overdot denotes derivatives with respect to the dimensionless time τ defined earlier.

2.9 Higher-order Feedback

Higher-order feedback terms do not play a significant role in Hopf bifurcation (Manmohan 1998) However, as will be seen later in this work, they play a crucial role in the study of static bifurcations. The higher-order terms of moderator are not considered in the present work. We describe below the higher-order feedback reactivity as follows.

$$\rho = \rho_{fb} = \rho_{fb}^{(1)} + \rho_{fb}^{(2)} + ..., \qquad (2.41)$$

with

$$\rho_{fb}^{(1)} = \alpha_f (T_f - T_{fo}) + \alpha_c (T_c - T_{co}) \ , \qquad (2.42)$$

$$\rho_{fb}^{(2)} = \alpha_F (T_f - T_{fo})^2 + \alpha_C (T_c - T_{co})^2 , \qquad (2.43)$$

where α_F and α_C denote the second order reactivity feedback coefficients for the fuel and the coolant , respectively, and the other symbols are as used earlier in this chapter. It is to be noted that the units of α_F and α_C are K^{-2}, while those of the linear feedback coefficients, α_f and α_c are K^{-1}. Introducing Eqs. 2.41-2.43 in Eq 2.1 , and making use of the nondimensional variables and parameters already defined, we can write the first equation in reactor kinetics as follows.

$$\frac{d\wp}{d\tau} = -\wp + \subset + a_f \Im_f + a_c \Im_c + a_f \wp \Im_f + a_c \wp \Im_c$$

$$+ a_F \Im_f^{\,2} + a_C \Im_c^{\,2} + a_F \wp \Im_f^{\,2} + a_C \wp \Im_c^{\,2} \qquad (2.44)$$

where

$$a_F = \alpha_F (T_{fo} - T_i)^2 / \beta,$$

$$a_C = \alpha_C (T_{co} - T_i)^2 / \beta,$$

and all other parameters are as defined earlier.

2.10 Control Reactivity Feedback

In this present work we consider a simple control model based on proportional and differential controllers. The control may be based on the fractional change in reactor power and / or a suitably defined fractional change in reactor coolant temperature. Thus the control reactivity ρ_c can be written as

$$\rho_c = K_p(\wp + t_p \frac{d\wp}{dt}) + K_c(\Im_c + t_c \frac{d\Im_c}{dt}) \qquad (2.45)$$

where

K_p = (negative) constant (gain) proportional to the fractional change in power represented by the dimensionless power $\wp$,

K_c = (negative) constant (gain) proportional to the fractional change in coolant temperature represented by dimensionless $\Im_c$, and

t_p, t_c = time constants associated with the differential controller based on the rate of change of power or coolant temperature respectively.

Inclusion of control reactivity changes only the first equation in the dynamical systems presented earlier. If the differential controller is included then the resulting equation is suitably recast by transferring the differential terms or substituting their values in terms of state variable from other equations.

The resulting equation governing the dimensionless power is given below :

$$(1-k_p\tau_p)\left[1-\frac{k_p\tau_p}{1-k_p\tau_p}\wp\right]\wp=(-1+k_p)\wp+\subset+(a_f+k_c\tau_c d)\Im_f+(a_c+k_c-k_c\tau_c d)\Im_c+a_m\Im_m$$

$$+\ \ldots\ldots\ldots \qquad (2.46)$$

where

$$k_p=\frac{K_p}{\beta}\ ,\quad k_c=\frac{K_c}{\beta}\ ,\quad \tau_p=\frac{t_p\beta}{\Lambda}\ ,\text{ and }\quad \tau_c=\frac{t_c\beta}{\Lambda}$$

Here only the linear terms on the RHS of Eq. 2.46 have been retained. As we will see later, analysis based on these linear terms show that bifurcation (static or dynamic) takes place for very large (negative) values of K_p or K_c, which are unlikely to occur in practice. As a result the higher-order terms on the RHS are not required in the present work.

2.11 Input Data

The set of input values that we need to know for each reactor model to carry out the analysis and computations have been arrived at in the preceding sections of this chapter. The input data are evaluated from the reactor data available from Power Reactors (1983) and World Nuclear Industry Handbook (1994). The fuel bundle and other data required for the standard 220 MWe and 500 MWe PHWR are taken from the AERB (1997); Bagchi (1994). Data of about 60 different PHWRs were grouped into 14 categories based on similarity of their operating and design features. Under different operating conditions, the input data can be widely different. The data for normal full power operation is summarized in Table 1.

Table 1: Input data† for PHWRs

Reactor	P_o	C_f	C_c	T_{fo}	T_{co}	T_{lo}
	MWt	MJK^{-1}	MJK^{-1}	K	K	K
220MWe-India	801	17.9	16.5	1313.5	544.0	522.0
500MWe-India	1725	35.8	41.3	1253.5	555.0	533.0
Bruce 1-4	2606	38.1	62.3	1438.0	547.5	522.0
Bruce 5-8	2832	38.1	67.7	1438.0	554.0	530.0
Cernavada 1-5	2180	26.7	52.1	1386.0	561.0	539.0
Darlington 1-4	2774	38.1	66.3	1423.0	562.5	538.0
Embaise-Cordoba	2103	27.4	50.3	1386.0	562.0	539.0
Gentilly 2	685	28.0	52.1	1386.0	561.0	539.0
Kanupp	433	9.72	8.91	1344.5	542.5	519.0
Pickering 1-8	1754	29.7	41.9	1430.5	544.4	522.0
Point Lepreau 1	2156	28.0	51.5	1386.0	561.5	540.0
Wolsong 1-2	2180	27.5	52.1	1386.0	561.3	539.6
Atucha 1	1179	12.4	24.3	1559.5	552.0	535.0
Atucha 2	2160	27.2	51.6	1559.5	567.9	550.5

† The meaning of each symbol is given in the Nomenclature and explained in the text.

Sample calculations of C_f and C_c for the 220 MWe are shown in Appendix A. The input data for the lumped parameter models of the moderator and steam generators is given in Table 2. A sample calculation for C_m is given in Appendix A. The value of C_s is taken to be One Full Power Second (FPS). The values of moderator temperatures are as given in Power Reactors (1983) and World Nuclear Industry Handbook (1994). The fraction of fission energy directly deposited in

the moderator (δ) is taken to be 5% in this work. The steady state SG secondary side temperatures based on the available data on the secondary side pressures (NPCIL 1992).

Table 2: Input data for the lumped parameter model of moderator and steam generator

Symbol	220MWe-India	500MWe-India
C_m	330 MJK^{-1}	840 MJK^{-1}
δ	0.05	0.05
T_{mo}	328 K	343 K
T_{mi}	318 K	328 K
α_m	-5×10^{-5} K^{-1}	-5×10^{-5} K^{-1}
C_s	1 FPS	1 FPS†
T_{so}	524 K	529 K

† The meaning of each symbol is given in the Nomenclature and explained in the text.

Table 3 gives input data, and the corresponding dimensionless parameter values used forone-group reactor kinetics. The dimensionless parameters are for the 220 MWe reactor.The coolant temperature coefficient α_c (or the corresponding dimensionless parameter a_c) is treated as the variable parameter in the PHWR models.

Tables 4 and 5 give six-group of delayed neutron data and the input constants and dimensionless parameters related to xenon and iodine (Lewins, 1978; Hetrick, 1971). The six-group data used is for thermal fission of uranium-235. The dimensionless parameters shown in Table 5 are for $\phi_0 = 10^{18}$ $m^{-2}s^{-1}$ and will change when a different steady state operating flux is considered. Fianlly

Table 6 lists the dimensionless thermal-hydraulic parameters (p,c,θ,q,r — all defined earlier) for the different categories / groups/ types of PHWRs considered in this work.

Table 3 : Input data and dimensionless parameters for one-group reactor kinetics

Input Values		Dimensionless Parameters	
Symbol	Value with Units	Symbol	Value
β	0.006	b	0.0075
λ	0.075 s^{-1}	a_f	-2.64
Λ	6.0 x 10^{-4} s	a_c	0.022
α_f	-2 x 10^{-5} K^{-1}	a_m	-2.65
α_c	6 x 10^{-6} K^{-1}		
α_m	-5 x 10^{-5} K^{-1}		

Table 4: Input data for six groups of delayed neutrons

Group i	Relative Yield a_i	Decay Constant λ_i (s^{-1})
1	0.038	0.0127
2	0.213	0.0317
3	0.188	0.115
4	0.407	0.311
5	0.128	1.40
6	0.026	3.87

Table 5 : Input data and dimensionless parameters for xenon and iodine

Input Data		Dimensionless Parameters (At $\nu = 2.5$, $\phi_0 = 10^{18}\ m^{-2}s^{-1}$)	
Symbol	Value with Units	Symbol	Value
γ_I	0.064	i	2.1742×10^{-6}
λ_i	$2.87 \times 10^{-5}\ s^{-1}$	x	1.5833×10^{-6}
γ_x	0.003	φ	13.9187
λ_x	$2.09 \times 10^{-5}\ s^{-1}$	γ	0.9552
σ_x	$2.70 \times 10^{-22}\ m^2$		

Table 6 : Dimensionless parameters' for PHWRs based on data given in Table 1

Reactor	p	c	θ	q	r
220MWe-India	0.005809	1.08606	0.027795	0.001192	0.005000
500MWe-India	0.006891	0.86884	0.030534	0.000685	0.003846
Bruce 1-4	0.007685	0.61113	0.027838	0.000947	0.005405
Bruce 5-8	0.008413	0.56248	0.026432	0.001535	0.003333
Cernavada 1-5	0.009830	0.51613	0.025974	0.000986	0.003125
Darlington 1-4	0.008466	0.57409	0.027684	0.001205	0.002985
Embaise-Cordoba	0.009304	0.54565	0.027155	0.000710	0.003030
Gentilly 2	0.002965	0.53763	0.025974	0.000318	0.000382
Kanupp	0.005555	1.09090	0.028468	0.000551	0.005405
Pickering 1-8	0.006660	0.70913	0.024656	0.000649	0.006494
Point Lepreau 1	0.009329	0.54395	0.025414	0.001012	0.003077
Wolsong 1-2	0.009605	0.52841	0.025638	0.000986	0.003096
Atucha 1	0.009430	0.51175	0.016593	0.001066	0.004348
Atucha 2	0.008000	0.52730	0.017245	0.001724	0.002571

† The meaning of each dimensionless parameter is given in the Nomenclature and explained in the text.

Chapter 3

Analytical and Computational Techniques

3.1 Operating Point Stability and Bifurcation Points

The steady stateof a linear system is determined by equating the rates of changes $\dot{X}$, to zero. Inevitably in a real system there will be small disturbances and we study the resulting transients. If these disturbances, whatever their inital form, die out, the system is stable. If they grow,or even if only some of them grow, the linearity implies that they will go on growing without bound ; the system is unstable. There is a possiblity of a behavior on the limit of stability, where an oscillatory behavior is maintained whose amplitude neither increases nor decreases from the initial disturbance.

The solution structure of the linearised system

$$\dot{X} = U(\eta)X$$

associated with the nonlinear dynamical system (Eq. 2.22) is determined by the eigenvalues and the corresponding eigenspaces of the Jacobian matrix U(η). As noted earlier $X_o = 0$ is an equilibrium or fixed point for the dynamical system for all values of η. For those values of η for which none of the eigenvalues of U(η) is on the imaginary axis, the fixed point is called *hyperbolic*. For these parameter values, the stability properties of the nonlinear system (Eq. 2.22) *locally* coincide with those of the linear system in some neighborhood of η. If for some $\eta = \eta^*$, some or more of the eigenvalues are on the imaginary axis, the equilibrium point is called *non-hyperbolic*. In the vicinity of η^* the stability properties of the system (Eq. 2.22) can only be understood by including the high-order nonlinear terms in the analysis. In such parameter-dependent systems, it is important to understand the qualitative behavior of the system as the parameter change. A bifurcation describes a qualitative change in the dynamics when the parameters in the system are varied. The values of the parameters where this change takes place are called critical values or bifurcation values. Knowledge of bifurcation values is absolutely essential for the complete understanding of the system. The best understood bifurcations are those for which a local analysis is possible. Among these, the most important bifurcations are of codimension one, i.e., bifurcations which are essentially one-parameter phenomena and can occur in a persistent way in a one dimensional parameter space (Bruno, 1989). In this chapter we examine the phenomena of Hopf bifurcation and static bifurcation in the dynamic models of the fission reactors of PHWR type, using a local analysis based on the theory of center manifold and normal forms (Wiggins, 1989; Guckenheimer and Holmes, 1983).

Hopf Bifurcation

A Hopf bifurcation occurs if for some $\eta = \eta^*$ (the critical or bifurcation value), there exits a pure imaginary pair of eigenvalues which crosses the imaginary axis transversally, as η is varied, while all the other eigenvalues remain in the left-half plane(Figure 2b). If the minimum dimension of the control parameter to be varied is one, we have a Hopf bifurcation of codimension one. Bifurcations of higher dimension are of less practical interest. At Hopf-

bifurcation, an equilibrium point bifurcates into limit cycles. A hopf bifurcation is also sometimes refereed to as a complex or dynamic bifurcation.

Static Bifurcation

A static bifurcation occurs if for some $\eta = \eta^*$ a zero eigenvalue crosses the imaginary axis through the origin as η is varied, while all other eigen values remain in left-half plane(Figure 2a).Saddle-node, transcritical and pitchfork are three types of static bifurcations. The type of bifurcation where on one side of a parameter value there are no fixed points and on the other side there are two fixed points is refered to as saddle-node bifurcation. If at the bifurcation point exchange of stability occurs then it refers to transcritical bifurcation. In pitchfork bifurcation, the operating fixed point which is stable becomes unstable creating two new stable fixed points at the bifuracating point. A static bifurcation is referred to as a real bifurcation.

A Hopf bifurcation is illustrated in Figures 4a,4b and 4c, while the the three types of static bifurcations are illustrated in Figure 3a, 3b and 3c.

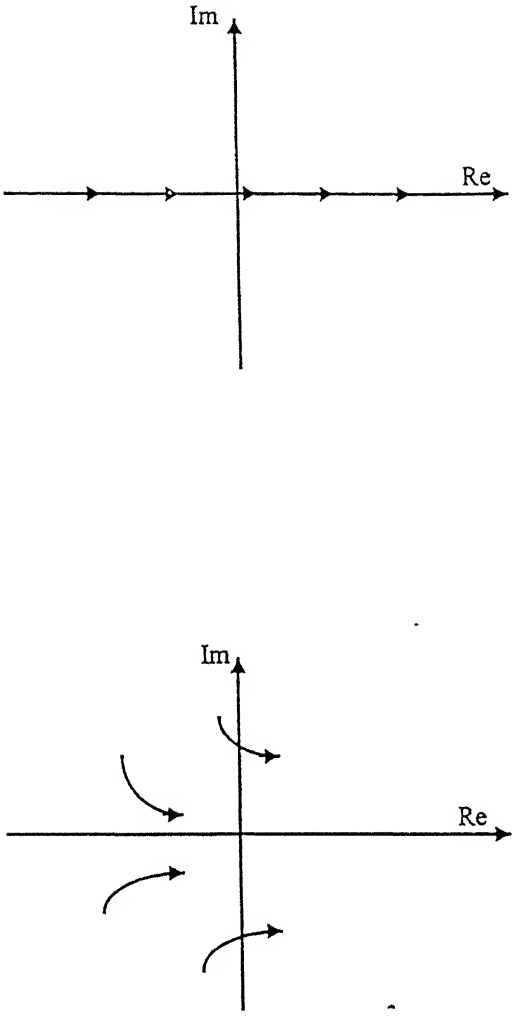

Figure 2 : A schematic diagram of (a) static bifurcation (b) hopf bifurcation

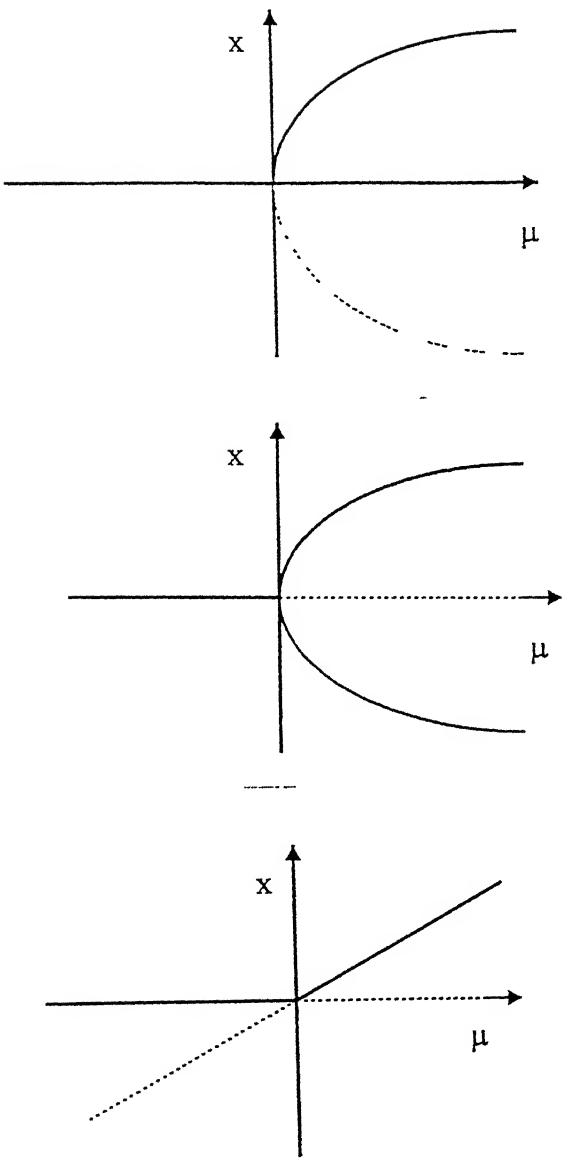

Figure 3: Schematic diagrams of (a) saddle-node (b) pitchfork and (c) transcritical bifurcations

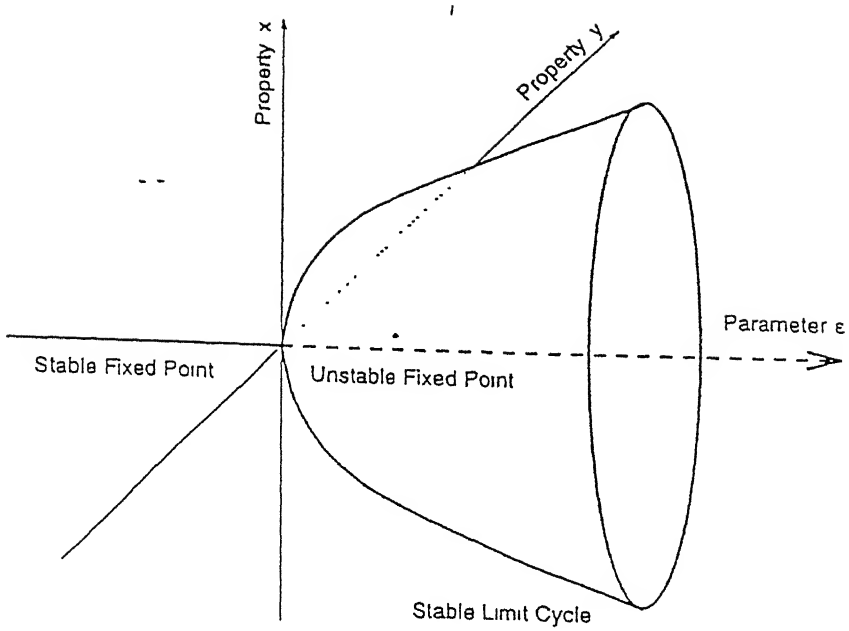

Figure 4 : (a) A schematic diagram of a normal (supercritical)Hopf bifurcation

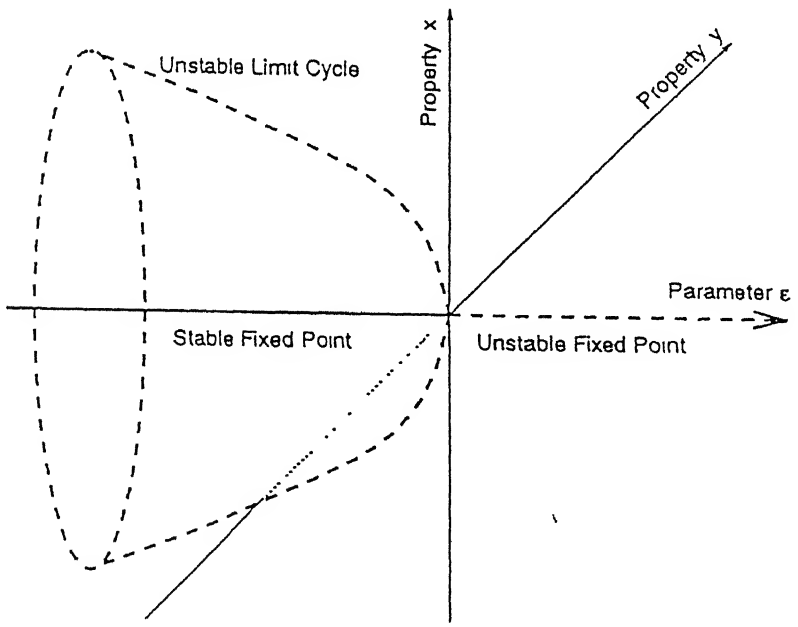

Figure 4 : (b) A schematic diagram of a subcritical (inverse) Hopf bifurcation

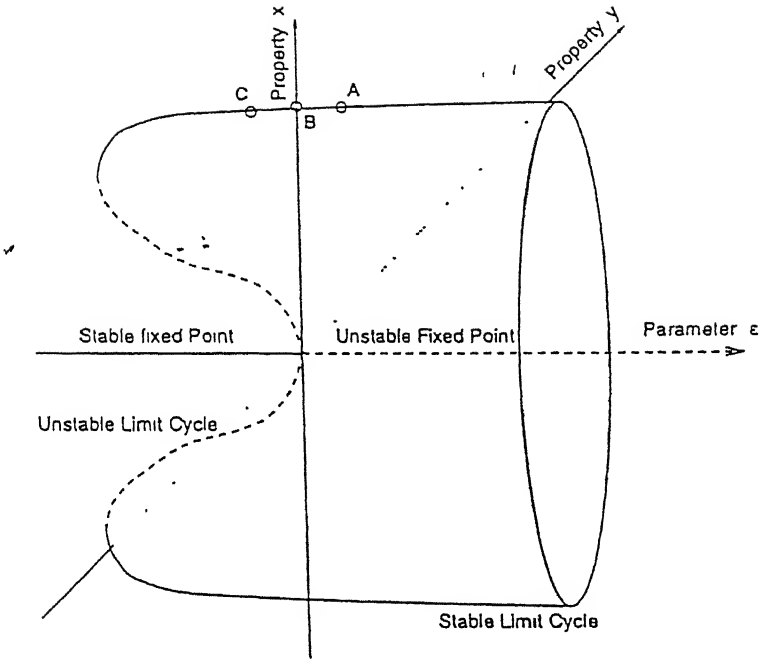

Figure 4 : (c) Coexistence of unstable and stable solutions in a subcritical Hopf bifurcation

3.2 Normal Forms at Bifurcation Points

Several analytical and computational techniques are needed to locate the bifurcation points and to investigate the behavior of the dynamical system in the vicinity of these points. These has been discussed in detail by Wiggins (1989) , Parker and Chua (1989), . The techniques required for the analysis of Hopf Bifurcation are also developed in Manmohan (1996). Below we summarize the methods used in the present work for the study of both the Static and Hopf Bifurcation in PHWR systems

Poincare Normal Form

A systematic way to ascertain the effect of the nonlinear terms is to reduce the dynamical system to a two dimensional center manifold, which is then transformed to the Poincare normal form. The proof that this can be done may be found in Wiggins (1989). Here, we state the main results related to the Poincare normal form and introduce some notations used in the calculations. The Poincare normal form in the cartesian coordinates, x_1 and x_2 for Hopf bifurcation, can be written as

$$x_1 = \alpha(\varepsilon)x_1 - \omega(\varepsilon)x_2 + [a(\varepsilon)x_1 - b(\varepsilon)x_2](x_1^2 + x_2^2) + \ldots\ldots \qquad (3.1)$$

$$x_2 = \omega(\varepsilon)x_1 + \alpha(\varepsilon)x_2 + [b(\varepsilon)x_1 + a(\varepsilon)x_2](x_1^2 + x_2^2) + \ldots\ldots \qquad (3.2)$$

where the normal form parameters $a(\varepsilon)$ and $b(\varepsilon)$ are defined for all sufficiently small ε. The parameter $a(0)$, called the *stability parameter*, determines the stability of bifurcating periodic solutions (Wiggins 1989):

(i) The case $a(0) < 0$: The bifurcation is normal (supercritical).

(ii) The case $a(0) > 0$: The bifurcation is inverse (subcritical).

Remark : A simple proof of the above statements, facilitated by considering Poincare normal form in polar coordinates, may be found in Wiggins (1989).

The Poincare normal forms for static bifurcation in Cartesian coordinates are as given below:

$$x = \varepsilon \pm x^2 \text{ (saddle-node)},$$

$$x = \varepsilon x \mp x^3 \text{ (pitchfork)},$$

$$x = \varepsilon x \mp x^2 \text{ (transcritical)}.$$

In the above equations ε is the variable parameter. Let $\mu \in \eta$, and μ^* be the value of μ at which the bifurcation occurs. Then ε is defined as

$$\varepsilon = \frac{\mu - \mu^*}{\mu^*}$$

3.3 Location of Bifurcation Points

Several techniques have been discussed in the literature for the location of the bifurcation point (Kubicek and Marek, 1983). In general the algorithms used are iterative in nature and make use of the Newton-Raphson method to find the critical value of the parameter.

The critical value μ^* of $\mu \in \eta$ is located by solving the equation

$$\alpha(\mu) = 0 \qquad (3.3)$$

where $\alpha(\mu)$ denotes the real part of a complex conjugate pair of eigenvalues of the matrix $U(\eta)$, evaluated at the steady state / equilibrium (operating) point.

The QR Method

The eigenvalues of the matrix $U(\eta)$ for a given set of parameter values are calculated using the QR algorithm. The Jacobian matrices associated with the dynamical systems studied in the present work are, in general, nonsymmetric. Since a nonsymmetric matrix may not be balanced, it is first replaced by a balanced matrix with identical eigenvalues (Press, et al., 1993). This reduces the sensitivity of the eigenvalues to rounding errors during numerical computations. The matrix is then reduced to a simpler Hessenberg form and the eigenvalues are calculated by using the standard QR algorithm applicable to real Hessenberg matrices.

Newton-Raphson Iteration

The Newton-Raphson algorithm is used to find the solution of Eq 3.3. Since the success of a locally convergent scheme depends critically on having a good first guess for the solution, it is desirable to use a globally convergent method which guarantees some progress towards the solution at each iteration. Perhaps the best strategy is to bracket the root and then refine it by a combination of the Newton-Raphson and the bisection methods. This keeps the root within the brackets while taking advantage of the rapid local convergence of the Newton-Raphson method. We have mostly used this kind of approach in this work.

3.4 Calculation of Center Manifolds

The center manifold theory provides a means for systematically reducing the dimension of the state space which needs to be considered while analyzing the bifurcation of a given type. The dynamical system becomes further simplified if we put the center manifold in a normal form. This is based on the idea of introducing successive coordinate transformations to simplify the analytic expression of the vector field on the center manifold. In fact mathematicians have proved that under fairly general conditions, the local theory of codimension one bifurcations

from a fixed or equilibrium point can be reduced to few archetypes (Ruelle, 1989; Berge, *et al.*, 1984). It then suffices to decide which of them fits a given problem in order to obtain a qualitative picture of the flow in the neighborhood of the bifurcation point.

The analysis based on the center manifold and normal form calculations is facilitated if the operating or steady state point is translated to the origin.

Hopf Bifurcation

Calculation of center manifolds and normal forms requires considerable amount of algebra, [referred to as *Horrendous* by Wiggins (1989)] particularly for the 2-dimensional Hopf bifurcation. These algebraic aspects are investigated in detail by Manmohan (1996) and in the present work we used the same computer program to determine the stability parameter, a(0), occurring in the Poincare normal form. We first consider the parameter independent case and let $U=U(\eta^*)$ and $W(X) = W(X, \eta^*)$ to simplify the notation.

In order to calculate the center manifold of the dynamical system

$$\dot{\mathbf{X}} = \mathbf{UX} + \mathbf{W(X)} \tag{3.4}$$

$$\text{let } \mathbf{X} = \mathbf{SY}$$

where S is the matrix whose columns are the eigenvectors of U. Thus we have

$$\dot{\mathbf{Y}} = (\mathbf{S}^{-1}\mathbf{US})\mathbf{Y} + \mathbf{S}^{-1}\mathbf{W(SY)} \tag{3.5}$$

$$= \Lambda\mathbf{Y} + \mathbf{S}^{-1}\mathbf{W(SY)} \tag{3.6}$$

Equation 3.2 can be separated into two parts :

$$\begin{aligned} \dot{u} &= \mathbf{A}u + \mathbf{F(u,v)} \\ \dot{v} &= \mathbf{B}v + \mathbf{G(u,v)} \end{aligned} \tag{3.7}$$

where

$$A = \begin{bmatrix} 0 & \omega_o \\ -\omega_o & 0 \end{bmatrix}, \qquad Y = \begin{bmatrix} u \\ v \end{bmatrix}$$

Then the introduction of another nonlinear transformation

$$v = h(u) \tag{3.8}$$

followed by elimination of quadratic terms in the resulting equations is required to obtain the Poincare normal form. For details reference should be made to Wiggins(1989). Manmohan(1996).

Static Bifurcation

The transformations required for the calculation of center manifold/normal form for static bifurcation are similar to those for the Hopf bifurcation, but considerably simpler due to one-dimensional nature of the manifold. We illustrate it using one-group [PHWR] model., The center manifold **u**, (3.7) is one-dimensional and we can write it as

$$\dot{u} = F(u,v)$$

$$\text{let } v_i = h_i(u), \qquad i=1,2,....,n-1.$$

$$= b_i u^2$$

As shown in Wiggins(1989), each $h_i(u)$ must satisfy

$$\frac{dh_i}{du} F(u,h(u)) - \Lambda_i h_i - G_i(u,h(u)) = 0, \qquad i = 1,2,...n\text{-}1. \tag{3.9}$$

where

$$\Lambda = \begin{bmatrix} 0 & . & . & . & . & 0 \\ . & \Lambda_1 & . & . & . & . \\ . & . & \Lambda_2 & . & . & . \\ . & . & . & . & . & . \\ . & . & . & . & . & . \\ 0 & . & . & . & . & \Lambda_{n-1} \end{bmatrix}$$ is a diagonal matrix.

It is straightforward to see that if only linear feedback is used solution of Eq. 3.9 yields,

$$b_i = 0, \quad i = 1,...,n-1.$$

Thus, the center manifold / normal form has no quadratic terms. If all b_i's are zero, and the original nonlinear terms in **W(X)** do not contain cubic terms (as is the case with linear feedback), the center manifold or normal form also do not contain any cubic terms.

Thus with linear feedback, all the three types of static bifurcation are ruled out, and the behavior of the nonlinear system remains divergent as would have been the case in the linear system. This is in conformity with the fact that, with linear feedback, no additional equilibrium (fixed) point originates from the operating point, i.e., (0,0,...0).

If higher-order feedback effect are present, then, as shown in sec-2.9, these introduce additional quadratic and cubic terms in the system (Eq. 2.44) . Due to this cubic terms, an additional equlibrium solution/fixed point of interest emerges. It is easy to see that without the SG, this fixed point is given by (using one group of delayed neutrons)

$$\wp = \subset = \Im_f = \Im_c = \Im_m = -\frac{a_f + a_c + a_m}{a_F + a_C + a_M}, \qquad (3.10)$$

and with the SG, the new fixed point is given by

$$\wp = \subset = \Im_m = 0, \quad \Im_f = \theta \Im_c, \quad \Im_c = -\frac{a_f \theta + a_c + a_m}{a_F \theta^2 + a_C + a_M}, \quad \Im_s = \Im_c \qquad (3.11)$$

In the nominal calculations presented in Chapter 4, we have taken $a_m = 0$

It is straight to see that the bifurcation point corresponds to

$$a_f + a_c + a_m = 0$$

or $$a_f \theta + a_c + a_m = 0$$

as the case may be. Thus the new fixed / equilibrium point represented by Eq. 3.14 or 3.15 originates from the origin, i.e., from the operating point. Since only one new fixed point bifurcates from the origin, it indicates transcritical bifurcation, and excluding the possibility of saddlenode and pitchfork bifurcations. (The saddle node bifurcation is also excluded from the fact that the original equilibrium point, (0,0,...0) does not remain stable beyond the bifurcation point). The fact that at the bifurcation point, exchange of stability occurs, is brought out in diagrams shown in Chapter 4.

As can been seen from Eq. 2.44, the higher-order feedback effects introduce into the system not only the cubic terms, but additional quadratic terms. As a result, the quadratic terms in the normal form, can no longer be zero and thus, the normal form will correspond to that of transcritical bifurcation.

3.5 Calculation of Trajectories

Calculation of trajectories by numerical integration is perhaps the most important and expensive task in the simulation of a dynamical system. It is also a prerequisite for the application of geometric tools or mathematical constructs such as Poincare sections, phase portraits and the calculation of characteristic multipliers or Lyapunov exponents.

Over the years, a large number of algorithms have been developed to approximate the behavior of a continuos-time system on a digital computer. A proper choice of the method and a careful application play a crucial role in the computational accuracy and efficiency. Among the available methods, the major practical choices are the single step methods, the multistep predictor-corrector methods, and the Bulirsch-Stoer extrapolation methods. The most popular among the single step methods are the Runge-Kutta methods. Both explicit and implicit implementations of the methods mentioned above are available in literature. The choice depends on the stiffness of the system to be integrated. In the present work an implicit implementation of Bulirsch-Stoer method given by Press, etal (1993) is used.

3.6 Poincare sections and Characteristic Multipliers

In order to simplify the phase space diagrams of a dynamical system of order n, one introduces an (n-1) dimensional surface of sections in the phase space and, instead of studying a complete trajectory, one monitors only the points of its intersection with this surface. A set of points of intersection of the trajectory with a hypersurface, as the trajectory crosses the surface from one side to the other, is referred to as *Poincare section.* Mapping an intersection point onto the subsequent intersection point is referred to as the *Poincare (return) map.*

The stability of periodic solutions or closed orbits is determined by the characteristic (Floquet) multipliers or roots. These can be regarded as a generalization of the eigenvalues at an equilibrium point. According to standard Floquet theory, the stability of a periodic orbit is determined by the eigenvalues of the monodromy matrix $\Phi(T)$ (also referred to as Floquet transition matrix), which is simply defined as the value of the fundamental matrix at the time period T, with the initial value as the unit matrix **I** (Kubicek and Marek 1983). If these eigenvalues lie within the unit circle in the complex plane, the periodic solution is stable. It is well known that one of the eigenvalues of $\Phi(T)$ is always unity (Husseyin, 1986; Parker and

Chua 1989). Thus a periodic orbit can never be asymptotically stable. The remaining eigen values of $\Phi(T)$ determine the *orbital* stability and are called the characteristic multipliers.

In the present work, we confirm the existence of limit cycles (whenever these occur) using Poincare sections, and calculate the characteristic multipliers using a method based on Poincare return maps (Manmohan 1996). The numerical results for both the transcritical and Hopf bifurcations are reported and discussed in the next chapter.

Chapter 4

Numerical Results, Discussion, and Conclusions

Numerical simulations are required to conform the predictions of the theoretical considerations given in Chapter 3. Furthermore, the theory is valid only in an arbitrarily small neighborhood of the bifurcation points. As one moves away from this neighborhood, numerical calculations are often the only means of obtaining information about the nature of the solutions. In this chapter, we present the numerical results for the lumped parameter PHWR dynamical systems developed in Chapter 2.

4.1 Stability at Full Power Operation

Before proceeding to calculate the critical values of the parameters for which the bifurcations may occur and simulating the behavior subsequent to bifurcation , it is desirable to confirm the stability of the systems considered at their normal operating values. In reactor dynamical systems, this indicated by the *reactor period,* T_p , or the e-folding time Glasstone (1994),

$$T_p = \left(\frac{P}{\frac{dP}{dt}} \right) \equiv \frac{1}{\omega_o},$$

where ω_o is the real part of the eigenvalue closest to the imaginary axis. The eigenvalues are calculated for the jacobian matrix U, (Eq. 2.22), evaluated at the normal operating point. A negative reactor period indicates stability at the point under consideration.

Table 7 shows the (negative) reactor periods for the reference PHWR (220 MWe) using five dynamical models presented in Chapter 2. It can be seen that for all the models (reactor periods are shown for the core, core along with moderator , core with moderator and SG), reactor stability is indicated at full power steady state operation. This is also the case for the other reactors studied. This is indicated in Table 8 using six groups of delayed neutrons.

Table 7: Reactor Period for full operation at full power for the Reference PHWR(220 MWe)

Reactor Model	Negative Reactor Period (s)		
	Core	Core + Moderator	Core + Moderator + SG
No delayed neutrons	32.7	81.95	1.18×10^3
Effective- lifetime model	35.4	81.75	1.18×10^3
Prompt-jump approximation	9.80	81.73	8.95×10^1
One group of delayed neutrons	9.77	81.73	1.18×10^3
Six groups of delayed neutrons	83.3	82.53	1.18×10^3

Table 8 : Reactor Periods at full power operation for the PHWRs shown in Table 1

(using six groups of delayed neutrons)

Reactor	Negative Reactor Period† (s)		
	Core	Core + Moderator	Core + Moderator + SG
220 MWe-India	8.33×10^{1}	8.25×10^{1}	1.18×10^{3}
500 MWe-India	8.33×10^{1}	1.39×10^{2}	1.11×10^{3}
Bruce 1-4	8.33×10^{1}	1.02×10^{2}	1.38×10^{3}
Bruce 5-8	8.33×10^{1}	8.32×10^{1}	1.37×10^{3}
Cernavada 1-5	8.34×10^{1}	9.71×10^{1}	1.29×10^{3}
Darlington 1-4	8.33×10^{1}	8.16×10^{1}	1.35×10^{3}
Embaise-Cordoba	8.34×10^{1}	1.19×10^{2}	1.29×10^{3}
Gentilly 2	8.30×10^{1}	3.02×10^{2}	1.37×10^{3}
Kanupp	8.33×10^{1}	1.18×10^{2}	1.22×10^{3}
Pickering 1-8	8.32×10^{1}	1.48×10^{2}	1.37×10^{3}
Point Lepreau 1	8.34×10^{1}	9.45×10^{1}	1.29×10^{3}
Wolsong 1-2	8.34×10^{1}	9.71×10^{1}	1.29×10^{3}
Atucha 1	8.32×10^{1}	9.04×10^{1}	1.55×10^{3}
Atucha 2	8.32×10^{1}	8.31×10^{1}	1.54×10^{3}

† A negative reactor period indicates stability at normal operating point of the reactor based on the data and reduced -order models used for the calculations.

The effect of different models of moderator and SG on reactor period is shown in Table 9 and unless otherwise specified, the models 2 of moderator and SG (Eqs. 2.5 and 2.9) are used along with the core in all the analysis.

Table 9 : Effect of different models of moderator and steam generator (SG) on reactor period for the reference reactor (220 MWe) (normal operation at full power using one group of delayed neutrons)

Moderator Model	SG model	Negative Reactor Period (s)
Constant heat removal rate	Constant secondary side temperature	2.64×10^3
	Constant power removal in the SG	7.91×10^2
Heat removal rate proportional to moderator temperature	Constant secondary side temperature	8.17×10^1
	Constant power removal in the SG	1.18×10^3

4.2 Critical Parameter Values

For the purpose of bifurcation studies, we have been treated the coolant temperature coefficient of reactivity , α_c , as the variable parameter, keeping all other parameters fixed. (A simultaneous variation of all parameters with a view to find the worst combination is presented later.) The

critical values, α^*_c, for the static and dynamic bifurcations for the reference reactor 220 MWe core are presented in Table 10 using

- No delayed neutrons
- Effective life time model
- Prompt-jump approximation
- One group of delayed neutrons
- Six groups of delayed neutrons

Table 10 : Critical Values of the coolant temperature coefficient of reactivity (α_c) for static and dynamic bifurcation for the Reference PHWR core

Reactor Model	Critical Values α^*_c K^{-1}	
	Static	Dynamic
No delayed neutrons	7.20×10^{-4}	-8.19×10^{-4}
Effective- lifetime model	7.20×10^{-4}	-8.48×10^{-3}
Prompt-jump approximation	7.20×10^{-4}	----------
One group of delayed neutrons	7.20×10^{-4}	-6.270×10^{-2}
Six groups of delayed neutrons	7.20×10^{-4}	-5.428×10^{-2}

It can be seen that the critical values for Hopf bifurcation considerably depend on the model employed. In fact the prompt-jump approximation does not give any critical value for the Hopf bifurcation. For this reason, unless otherwise indicated, we have used one-group and six-group models only.

The effect of moderator and SG on the critical value, α^*_c, is brought in Tables 11 and 12, for the static and Hopf bifurcations respectively, using one and six groups of delayed neutrons. While the effect of the number of groups of delayed neutrons is relatively small, the effect of moderator and SG on the critical value is considerable.

Table 11 : Effect of moderator and steam generator (SG) on the critical values of α_c for the static bifurcation in PHWR (220 MWe)

Core Model	Critical Values α^*_c (static), K^{-1}		
	Core	Core + Moderator	Core + Moderator + SG
One group of delayed neutrons	7.20×10^{-4}	7.42×10^{-4}	2.0×10^{-5}
Six group of delayed neutrons	7.20×10^{-4}	7.42×10^{-4}	2.0×10^{-5}

It is observed that xenon destroys the possibility of static bifurcation by introducing a complex eigenvalue at the bifurcation point. Hence its effect only on dynamic bifurcation is studied using PHWR (220 MWe) along with moderator and SG using one and six groups of delayed neutrons. This is shown in Table 13. For comparison the critical values without the effect of xenon on dynamic bifurcation are also presented in Table 13. It can be seen that the effect of xenon on the critical values is negligible.

Table 12 : Effect of moderator and steam generator (SG) on the critical values of α_c for the dynamic bifurcation in PHWR (220 MWe)

Core Model	Critical Values α^*_c (dynamic) , K^{-1}		
	Core	Core + Moderator	Core + Moderator + SG
One group of delayed neutrons	-6.269×10^{-2}	-6.2720×10^{-2}	-6.9662×10^{-2}
Six group of delayed neutrons	-5.442×10^{-2}	-5.4303×10^{-2}	-6.1063×10^{-2}

Table 13: Effect of xenon on the critical values of α_c for dynamic bifurcation in PHWR (220 MWe) (Core + Moderator + SG)

Core Model	Critical Values $\alpha^*_c \cdot K^{-1}$	
	Without Xenon	With Xenon
One group of delayed neutrons	-6.9662×10^{-2}	-6.9640×10^{-2}
Six group of delayed neutrons	-6.1063×10^{-2}	-6.1040×10^{-2}

Table 14 shows the critical values for the other reactors using one group of delayed neutrons and including the moderator and SG in the model. It can be seen from Tables 10 to 14, that the static (transcritical) bifurcation occurs for the positive values of the coolant temperature coefficient of reactivity (α_c), while the dynamic (Hopf) bifurcation occurs for the negative values of the same. Since the physical value of α_c is positive in PHWRs (under most operating conditions), the Hopf bifurcation is unlikely to occur. Even under those operating conditions where α_c may be negative, its magnitude is likely to be much smaller than that required for the Hopf bifurcation. which is of the order of -10^{-2} K^{-1} in all the reactors considered. The static bifurcation in these reactors occurs for the positive values of α_c of the order 10^{-3} to 10^{-4} K^{-1}, while the actual values is of the order 10^{-5} to 10^{-6} K^{-1}.

Table 14: Critical Values of coolant temperature coefficient of reactivity α_c for static and dynamic bifurcations for the PHWRs listed in Table 1(Core +Moderator) using one-group of delayed neutrons

Reactor	Critical Values α^*_c K^{-1}	
	Static	Dynamic
220MWe-India	7.22×10^{-4}	-6.2720×10^{-2}
500MWe-India	6.86×10^{-4}	-5.2701×10^{-2}
Bruce 1-4	7.48×10^{-4}	-4.1681×10^{-2}
Bruce 5-8	7.78×10^{-4}	-4.0991×10^{-2}
Cernavada 1-5	8.04×10^{-4}	-3.9009×10^{-2}
Darlington 1-4	7.53×10^{-4}	-3.9867×10^{-2}
Embaise-Cordoba	7.69×10^{-4}	-3.9072×10^{-2}
Gentilly 2	7.89×10^{-4}	-1.0634×10^{-1}
Kanupp	7.24×10^{-4}	-6.0857×10^{-2}
Pickering 1-8	8.41×10^{-4}	-5.3829×10^{-2}
Point Lepreau 1	8.22×10^{-4}	-4.1739×10^{-2}
Wolsong 1-2	8.15×10^{-4}	-4.0335×10^{-2}
Atucha 1	1.25×10^{-3}	-5.4412×10^{-2}
Atucha 2	1.20×10^{-3}	-6.0289×10^{-2}

4.3 Simultaneous Variation of Parameters

As we have seen above, in each of the reactors studied, bifurcations occur for possibly unrealistic values if the parameters other than α_c are considered constants. In this section we vary other dimensionless parameters in certain ranges, with a view to find those sets of parameters for which bifurcations may occur for values of α_c more likely to occur in practice. The dimensionless parameters due to xenon are not considered for the random parameter variation as it was seen from Table 13 that the effect of xenon on dynamic bifurcations is very small and hence the effect of xenon is not considered in future analysis. For this purpose the values attained by the dimensionless parameters for the 220 MWe reactor are treated as reference values and denoted by subscript R. These are reproduced in Table 15 along with the ranges explored for each parameter. The ranges are selected with the help of Table 6, with a view to allow for the worst-case combination. The actual values tried as given in Table 15, are broader than those suggested by Table 6.

Table 15 : Ranges of parameter ratios allowed for the worst case PHWR

Reference Value†		Parameter Ratio	Range	
			Lower limit	Upper limit
a_{fR}	-2.64	a_f / a_{fR}	1.0	0.25
a_{mR}	-2.65	a_m / a_{mR}	2.0	0.2
b_R	0.0075	b / b_R	0.3	3.0
c_R	1.08606	c / c_R	0.5	1.25
θ_R	0.02779	θ / θ_R	0.5	1.25
p_R	0.00580	p / p_R	0.01	10
q / p	0.00119	q / p	0.2	5.0
r / p	0.00500	r / p	0.2	5.0

† Reference values are for 220 MWe as given in Tables 2 and 6 and are here denoted by a subscript R .

The worst-case combination of parameters is found using random trials. The results are shown in Tables 16 and 17 for static and Hopf bifurcations respectively, together with the corresponding values of α^*_c .

Table 16: Values of the parameter ratios for the worst case PHWR for the static bifurcation within the ranges/ limits given in Table 15

Parameter Ratio	Worst-case value for the static bifurcation
a_f / a_{fR}	0.25
a_m / a_{mR}	-0,2
b / b_R	3.0
c / c_R	1.25
θ / θ_R	0.5
p / p_R	10.0
q / p	5.0
r / p	5.0
α^*_c (Core)	$1.7989 \times 10^{-4}\ K^{-1}$
α^*_c (Core + Moderator)	$1.7534 \times 10^{-4}\ K^{-1}$
α^*_c (Core + Moderator + SG)	$2.5 \times 10^{-6}\ K^{-1}$

Table 17: Values of the parameter ratios for the worst case PHWR for the dynamic bifurcation within the ranges / limits given in Table 15

Parameter Ratios	Worst-case value for the dynamic bifurcation		
	$\alpha_m = 0$	α_m = +ve	α_m = -ve
a_f / a_{fR}	0.25	0.25	0.25
a_m / a_{mR}	----	-0.2	2.0
b / b_R	3.0	3.0	3.0
c / c_R	0.570	0.5	1.333
θ / θ_R	1.25	0.5	0.5
p / p_R	0.01	0.01	10.0
q / p	----	5.0	0.2
α^*_c (K^{-1}) (one-group)	-4.107×10^{-5}	-6.068×10^{-5}	$+2.122 \times 10^{-4}$

In the worst-case the values of the coolant temperature coefficient of reactivity for which a static bifurcation is more likely to occur are found to be of the order of $+10^{-6}$ K^{-1}. While this value is physically realistic for PHWRs, It must be noted that this applies when the parameters of all reactors are combined in the worst manner. Table 17 also shows the effect of moderator feedback on dynamic bifurcation. Even though the physical value of moderator temperature coefficient of reactivity (α_m) for all PHWRs in the present work is taken to be negative, we have allowed a small positive value for the moderator temperature coefficient while exploring the ranges for the dimensionless parameters, as can be seen from Table 15. From Table 17 it is clear that the worst-case parameters depend strongly on the moderator temperature coefficient of reactivity.

The worst-case values of α^*_c in case of dynamic bifurcation range from -4 x 10^{-5} to +2 x10^{-4} K^{-1}, depending on the moderator temperatue coefficient of reactivity.

4.4 Trajectories, Bifurcation Diagrams and Phase Portraits

In this section , we present numerically simulated trajectories and bifurcation diagrams for the worst case and for the 220 and 500 MWe. Furthermore, as has been mentioned in Section 3.4 the static bifurcation is possible only when the higher-order feedback effects are also present. In the figures that follow, these effects are included for the transcritical bifurcation shown. In the case of Hopf bifurcation, we have ignored the higher-order feedback effects.

Figures 5 to 7 shows the time- response for the dimensionless power, and fuel and coolant temperatures subsequent to the transcritical bifurcation. The parameter values for which the figures are plotted are shown on the figures. It can be seen that while the behavior of the linear system, or the system with linear feedback, is divergent as expected, the behavior becomes bounded, as soon as any of the higher-order feedback effect is included. The presence of the new equilibrium point is indicated by the asymptotic approach to the same in Figures 5 to 7.

The actual values of the new equilibrium point depend on how far the parameter is from the bifurcation point. This is shown in Figures 8 to 10, where

$$\text{Epsilon} \equiv \varepsilon \equiv \frac{\alpha_c - \alpha_c^*}{\alpha_c^*} .$$

The exchange of stability between the operating point and the new fixed point at the bifurcation is also clearly visible in the figures. The solid curves represent stability while the dashed curves represent instability.

It should however be mentioned that new equilibrium point is only locally stable (in accordance with the local bifurcation theory). Thus all disturbed situations from the original operating point need not be in the basin of attraction of the new fixed point. The behavior shown in Figures 5 to 7 is valid only for those disturbances which are in the basin of attraction of the new equilibrium point. For other disturbances, the reactor behavior will remain divergent.

Figures 11 to 14 show the behavior subsequent to Hopf bifurcation in the worst-case PHWR dynamical system using one group of delayed neutrons. As has already been mentioned , the values of the parameters for which this behavior occurs appear to be impractical. These figures , however confirm the prediction of the theory predicted in Chapter 3. Figures 15 to 18 show the behavior subsequent to Hopf bifurcation in 220 and 500 MWe PHWRs for the core, core along with moderator, and core along with moderator and SG, using one group of delayed neutrons. In figures only two curves are seen as the curve for the core, and core with moderator overlap. We reemphasize that for 220 and 500 MWe reactors, the values of α^*_c (Table 14) for which the Hopf bifurcations are even more unphysical than those for the worst case (Table 17). However, even in this unlikely situation, while the dimensionless power variation during the limit cycles oscillation is large, its effect on fuel and coolant temperature is quite limited (1 to 5% for 200 and 500 MWe reactors, and ~ 15% when the parameters are combined in the worst manner for *all* the reactors listed in Table 6).

The stability of the limit cycles represented in Figures 11 to 14 is further confirmed by the calculation of stability parameter, a, and the characteristic multipliers shown in Table 18.
We mentioned here that as $a > 0$, the situation similar to that shown in Figure 3c occurs in these models. In view of the unphysical nature of α^*_c , we have not further investigated the coexistence of stable and unstable limit cycle in the vicinity of bifurcation point. This and its associated effects are reported in detail by Manmohan (1996) in the contexts of PWRs and BWRs.

Table 18: The stability parameter $a(0)$ and the characteristic (Floquet) multipliers for the PHWR core limit cycle (worst case)

Parameter	One Group	Six Groups
Stability Parmeter,a(0)	3.191×10^{-6}	1.632×10^{-5}
Floquet Multipliers ($\epsilon = 0.2$)	0.909 1.09×10^{-4} 3.30×10^{-6}	0.832 7.14×10^{-5} 1.76×10^{-6} 1.28×10^{-7} 9.33×10^{-8} 3.48×10^{-8} 1.73×10^{-8} 1.13×10^{-9}

4.5 Critical Values for the Control Reactivity

As given in Section 2.10 , the control may be based on the fractional change in reactor power and / or a suitably defined fractional change in reactor coolant temperature. Table 19 gives the critical values, α^*_c , for different values of K_p and t_p , as compared to the situation without control ($K_p = 0$, $t_p = 0$). It can be seen that bifurcation becomes all the more unlikely for all values of $K_p < 0$, the only situation that can occur in practice.

Table 19: Critical values of the coolant temperature coefficient of reactivity (α_c) for different values of K_p and t_p for the Reference Reactor (220 MWe : Core + moderator + SG) using 6 groups of delayed of neutrons

K_p	t_p	Critical values, α^*_c, K^{-1}	
		Static	Dynamic
0	----	2×10^{-5}	-6.11×10^{-2}
-0.1	0	2×10^{-5}	-1.71×10^{1}
	0.1	3.53×10^{-4}	-1.078
-10	0	2×10^{-5}	-1.53×10^{3}
	0.1	3.35×10^{-3}	-1.02×10^{1}

Table 20 shows the critical values of K_c for different values of t_c . It is seen that K^*_c is of the order of -1. This, for the values of T_{co}, T_{io} and β given in Tables 1 and 3 amounts to a coolant reativity feedback of the order of -10 $ per degree rise of D_2O coolant temperature. A practical value for the same which is likely to be of the order of -10^{-1} to 10^{-2} $ per degree rise in coolant temperature. Thus it can be concluded that control system is unlikely to introduce any kind of bifurcation.

Table 20 : Critical values of the control parameter K_c ($K_p = 0$, $t_p = 0$) for Hopf bifurcation in Reference PHWR(220 MWe)

t_c	K^*_c
0	-1.22
0.001	-1.24
0.01	-1.40

4.6 Conclusions And Observations

As summarized in the preceding sections, an analysis of Hopf bifurcation and static (transcritical) bifurcation in some models of PHWR dynamical systems has been presented in this work. Based on the analytical and numerical results , the following conclusions are drawn:

- Hopf and transcritical bifurcations in the models considered occur in one-dimensional parameter space, i.e., it is of codimension one. In general, the critical values of the variable parameter calculated using different mathematical models are found to differ considerably from each other. This is particularly so if the models based on the effective-lifetime and prompt-jump approximation are used and hence these models should not to be used for bifurcation studies. It is pointed out in this work that qualitatively, the behavior of the models with six groups of delayed neutrons is similar to that of the one-group models.

- In lumped parameter PHWR dynamical systems based on the two temperature feedback model and the parameter ranges explored, it appears that a PHWR core may be an unlikely

candidate to experience a Hopf bifurcation instability. This remains true for all (negative) gains in the proportional controllers and any time constants associated with the differential controllers. Effect of xenon is seen to be very low and hence its effect is omitted in the analysis of the present work. However, when the moderator feedback is included, for negative moderator temperature coefficient of reactivity α_m worst-case analysis shows that the likelihood of Hopf bifurcation is somewhat increased. This is not the case for the original three-temperature feedback PHWR model for any of the reactors.

- Static or transcritical bifurcation can occur only if the higher-order feedback coefficients are present. Of the three types of static bifurcation , it is shown in this work that only transcritical bifurcation can occur. The static bifurcation occurs for the positive values of α_c and is of the order of 10^{-3} to 10^{-4} K^{-1}, while the actual values is of the order 10^{-5} to 10^{-6} K^{-1}. For the worst-case, the critical value of α_c for the core along with the moderator and SG is of the order of 10^{-6} K^{-1}. However this is so if all the parameters are combined in the worst possible manner, an unlikely situation to occur in practice.

- It is noted in the present work that subsequent to transcritical bifurcation, the new equilibrium point is only locally stable and may not be an attractor for the all disturbances from the normal operating condition. Thus there remain disturbances of the operating condition from which the reactor will show unstable divergent behavior inspite of the presence of higher-order feedback coefficients.

A few observations and suggestions which may be useful in future extensions of the present work are given below:

- We have used space-independent lumped parameter models for the present study. It would be desirable to extend this study to include spatial effects.

- In present work, the control reactivity whether based on the change in reactor power or based on the change in coolant temperature, is assumed to act instantly. In future studies. appropriate governing equations for the control reactivity insertion should be included.
- The present study has been restricted to long-term or asymptotic behavior in the dynamical systems studied. The role of nonlinearities in the transients, which may sometimes last very long and whose behavior may be important in fission reactor dynamics and safety, should be include in future studies. This may also have an important bearing on the optimal design of the controllers / control law.
- In the present work, we have studied the local behavior in the vicinity of the bifurcation points. A global analysis may be attempted in future studies.
- Nonlinearities also effect the transient behavior of the reactor under normal operating parameter values. Their effect on the transients may have an important bearing on the optimal design of the controllers / control law. This can be a fruitful exercise to undertake in future.

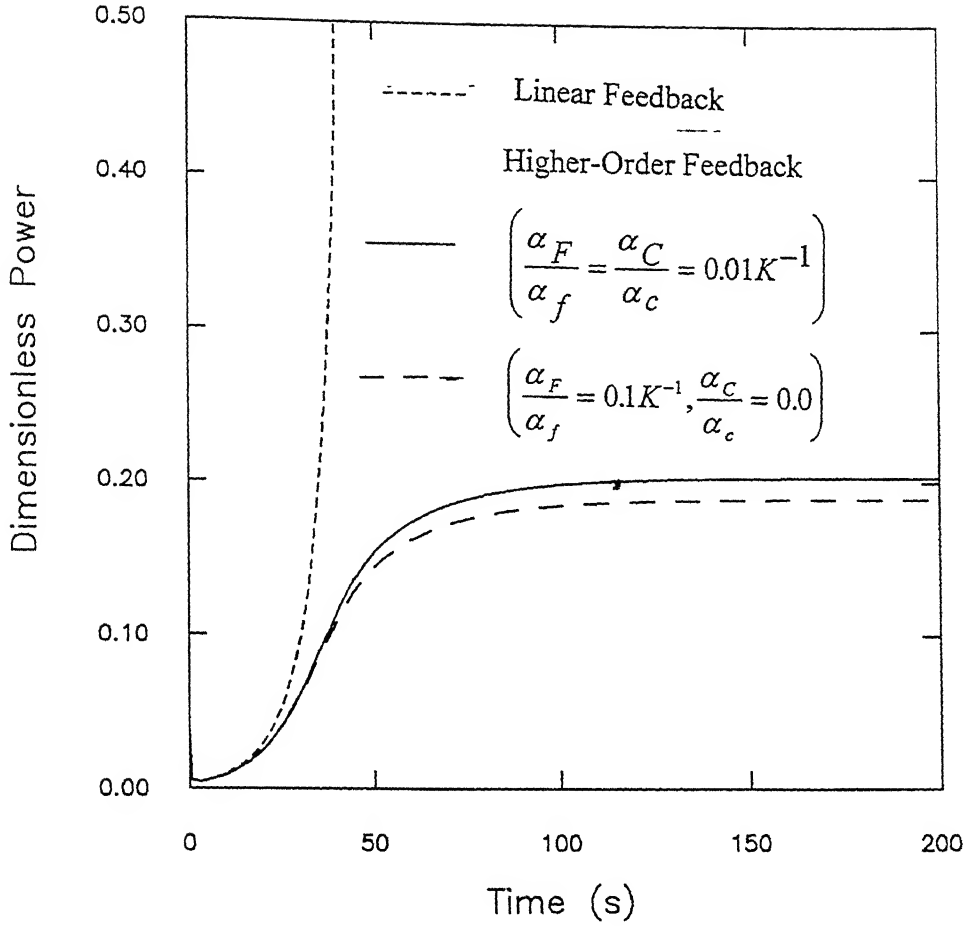

Figure 5: Time variation of dimensionless power $\wp$ subsequent to transcritical bifurcation in a PHWR core (worst case)

$$\left(\alpha_c=(1+\varepsilon)\alpha_c^*,\varepsilon=1.5,\alpha_c^*=1.80\times10^{-4}\,K^{-1}\right)$$

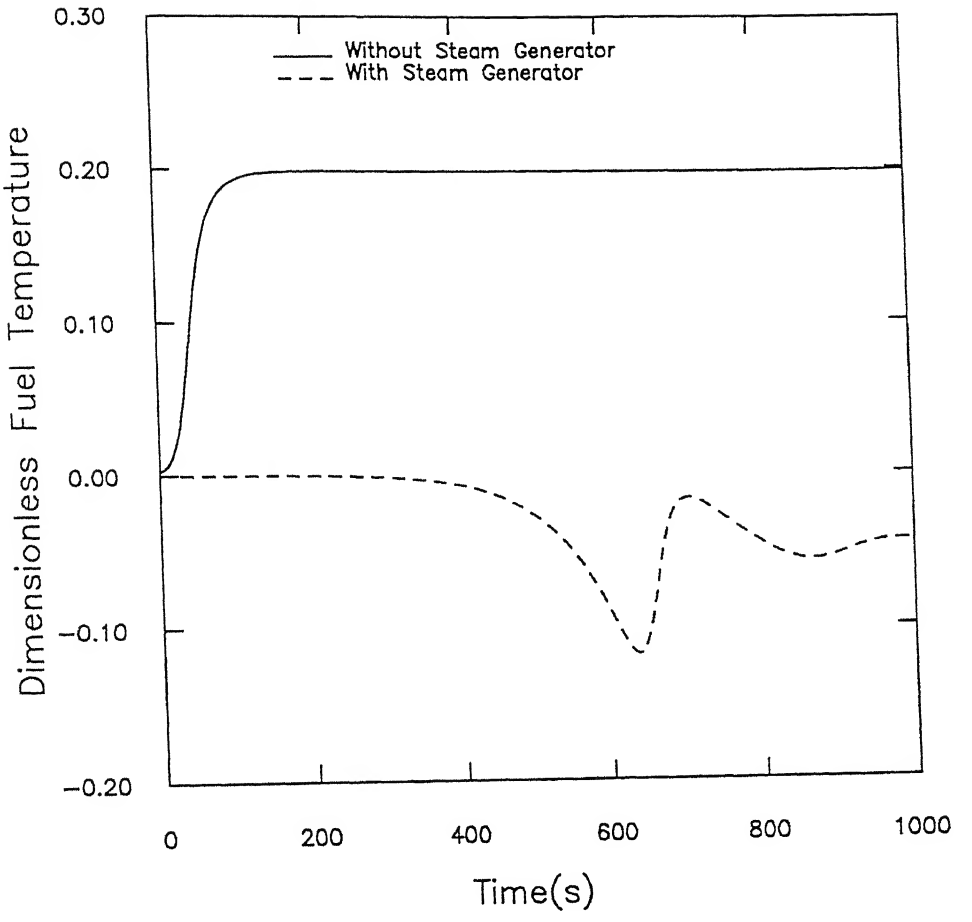

Figure 6 : Effect of Steam Generator on time variation of dimensionless fuel temperature $\Im_f$ subsequent to transcritical bifurcation using one-group of delayed neutrons in PHWR core with moderator (worst case)

$$\left(\varepsilon = 1.5, \frac{\alpha_F}{\alpha_f} = \frac{\alpha_C}{\alpha_c} = 0.01K^{-1} \right)$$

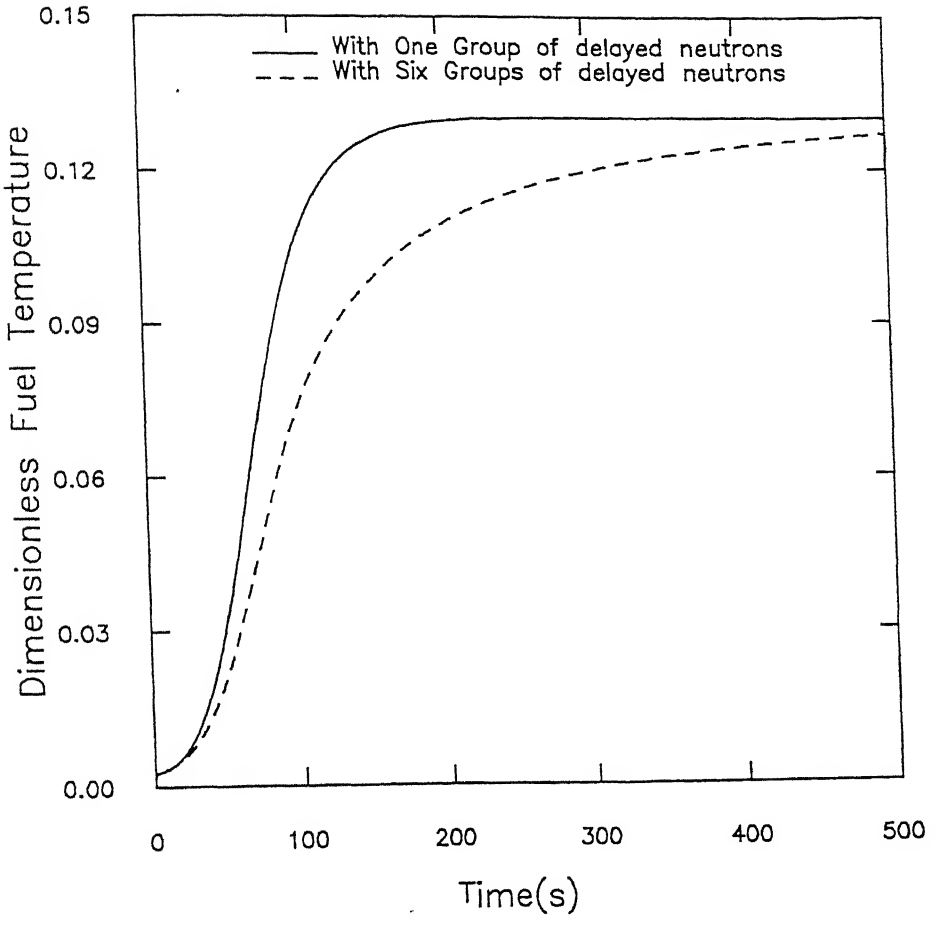

Figure 7: Effect of one and six groups of delayed neutrons on time variation of dimensionless fuel temperature $\Im_f$ subsequent to transcritical temperature in PHWR core with moderator

$$\left(\varepsilon = 1.0, \frac{\alpha_F}{\alpha_f} = \frac{\alpha_C}{\alpha_c} = 0.01K^{-1}\right)$$

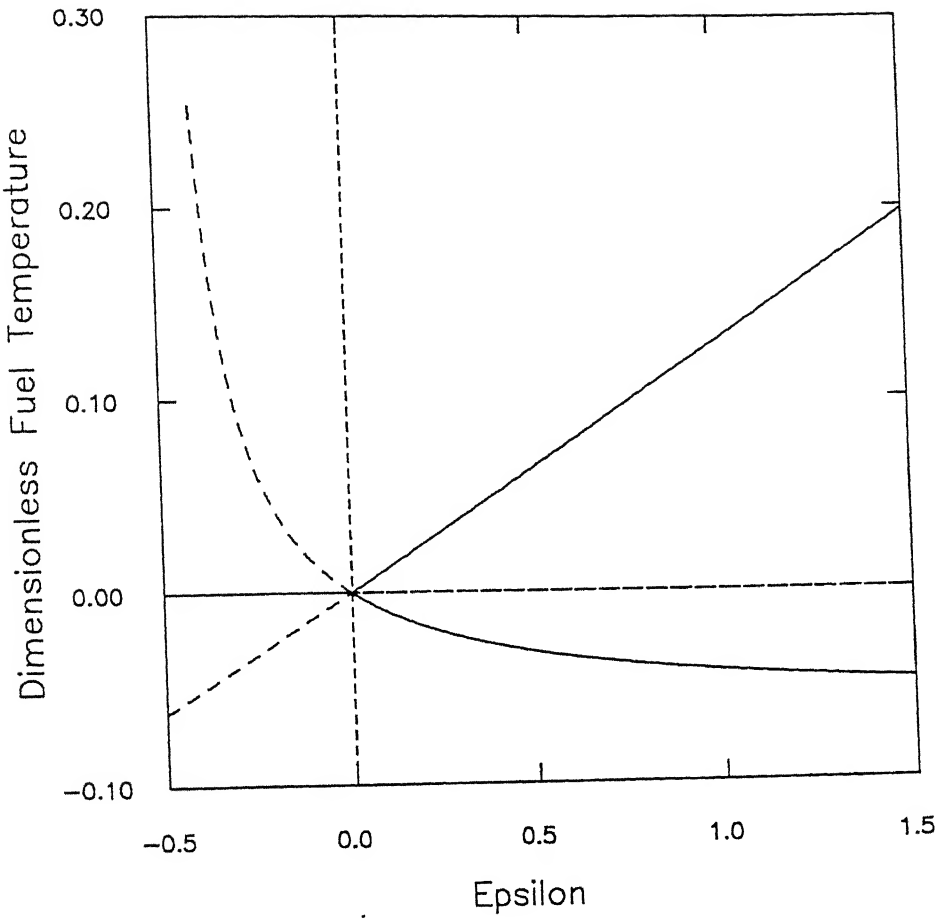

Figure 8 : Bifurcation diagram (with and without Steam Generator) for transcritical bifurcation in the worst case PHWR

$$\left(\frac{\alpha_F}{\alpha_f} = \frac{\alpha_C}{\alpha_c} = 0.01K^{-1}\right)$$

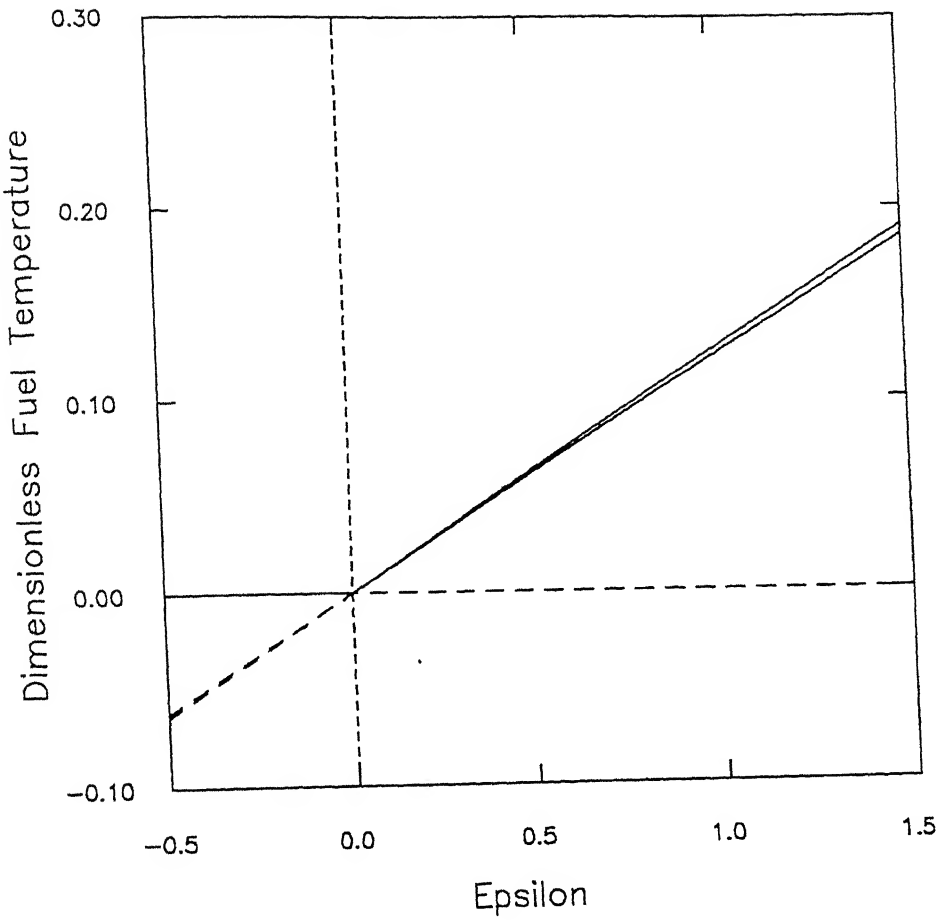

Figure 9 : Bifurcation diagram (with and without Steam Generator) for transcritical bifurcation in the worst case PHWR

$$\left(\frac{\alpha_F}{\alpha_f} = 0.0, \frac{\alpha_C}{\alpha_c} = 0.01K^{-1}\right)$$

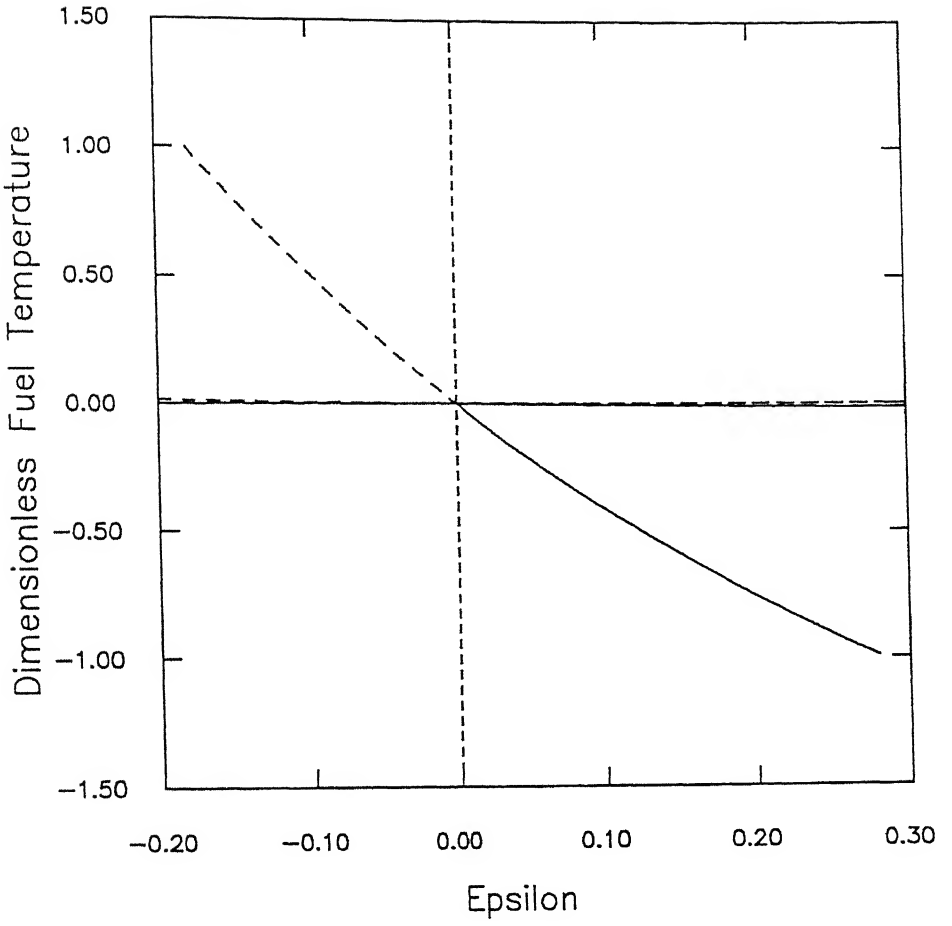

Figure 10 : Bifurcation diagram (with and without Steam Generator) for transcritical bifurcation in the worst case PHWR

$$\left(\frac{\alpha_F}{\alpha_f} = 0.01K^{-1}, \frac{\alpha_C}{\alpha_c} = 0.0\right)$$

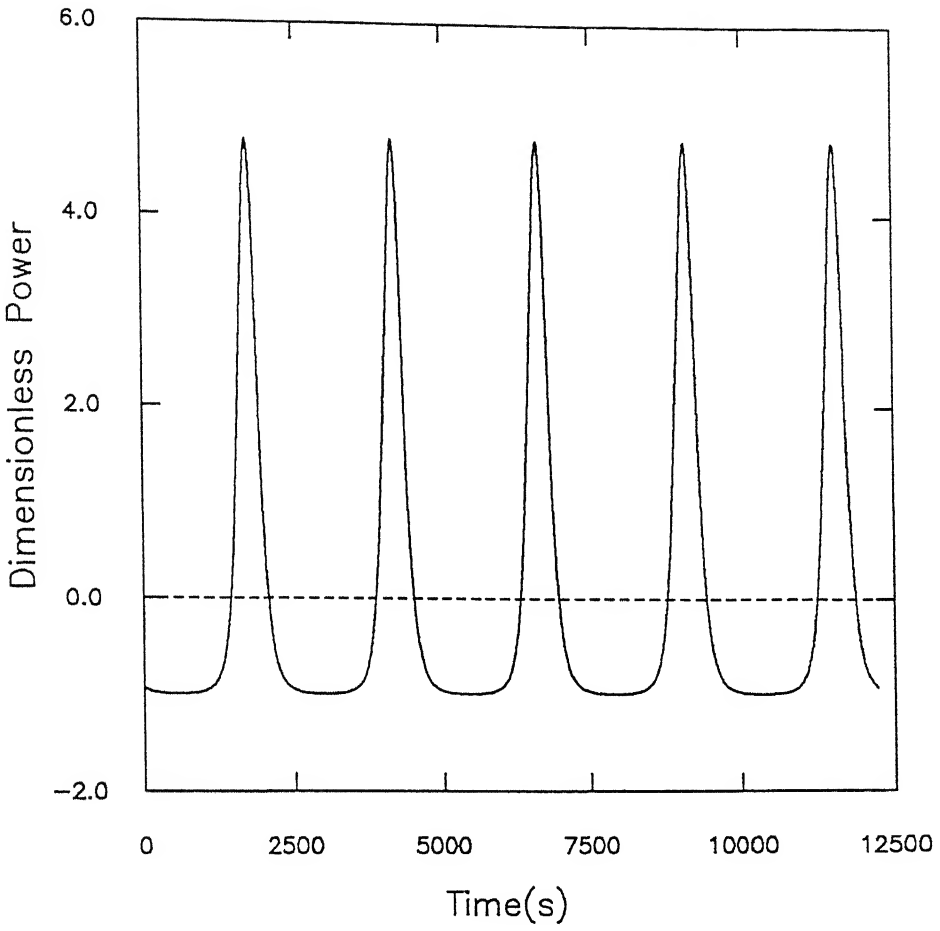

Figure 11 : Behavior of Dimensionless Power (neutron flux) versus time in PHWR core (worst case) subsequent to Hopf bifurcation using one-group of delayed neutrons ($\varepsilon = 0.2$)

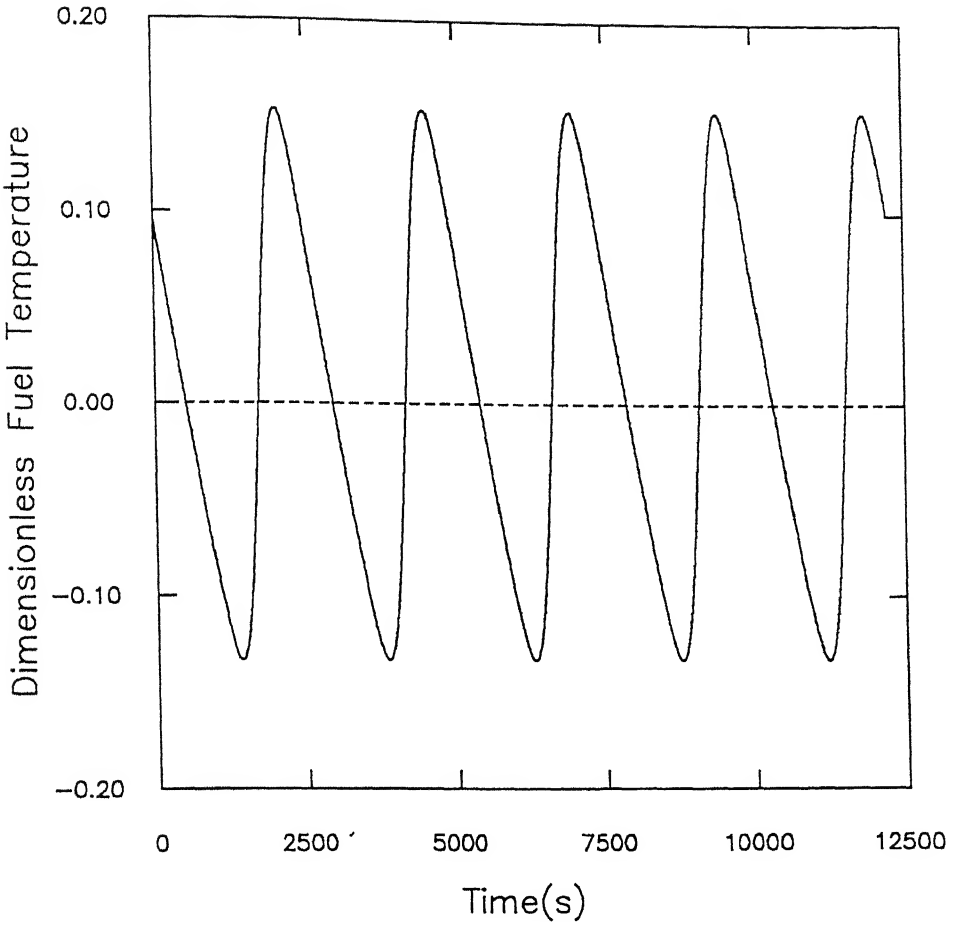

Figure 12 : Behavior of Dimensionless coolant temperature (neutron flux) versus time in PHWR core (worst case) subsequent to Hopf bifurcation using one-group of delayed neutrons ($\varepsilon = 0.2$)

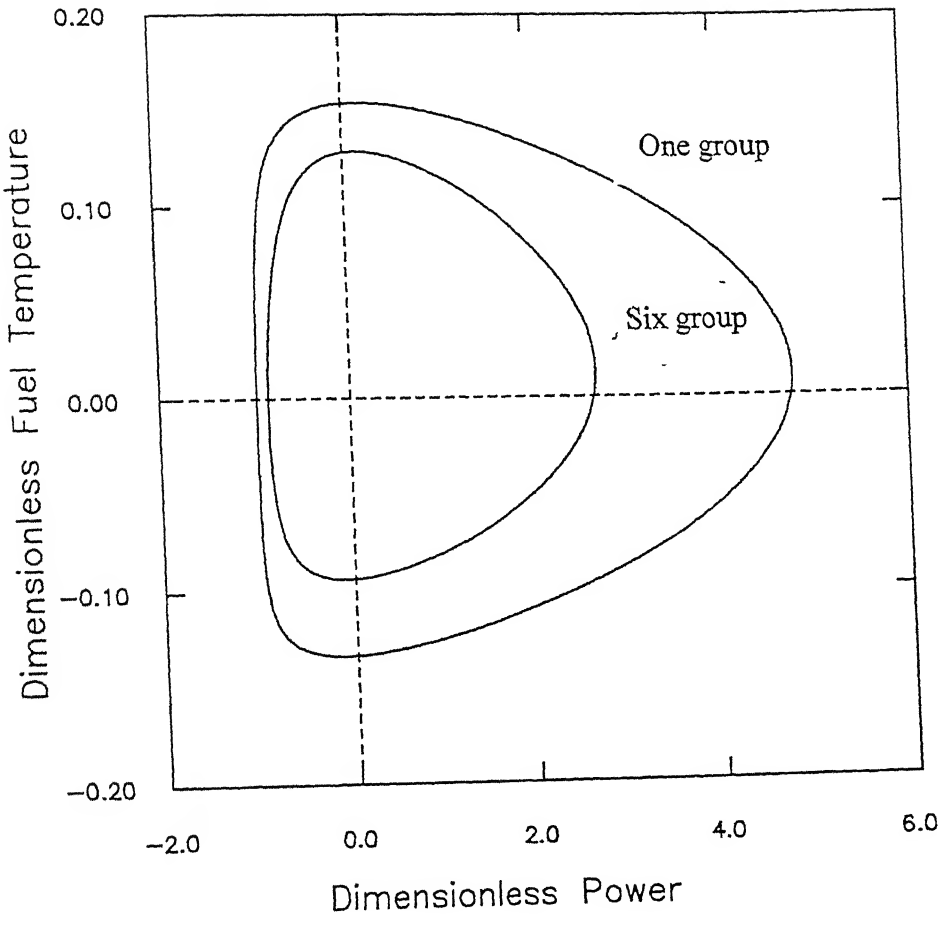

Figure 13 : Phase portrait of limit cycles in PHWR core with moderator(worst case) on $\wp - \Im_f$ plane subsequent to Hopf bifurcation ($\varepsilon = 0.2$)

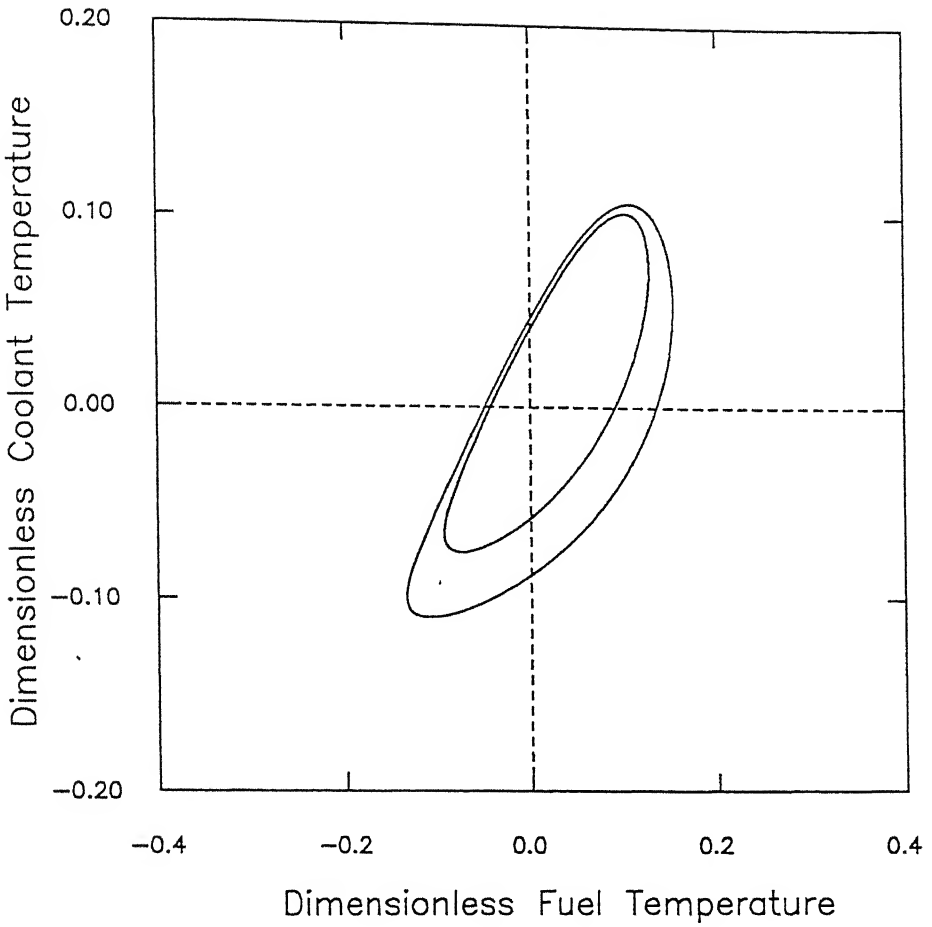

Figure 14 : Phase portrait of limit cycles in PHWR core with moderator(worst case) on $\Im_f - \Im_c$ plane subsequent to Hopf bifurcation ($\varepsilon = 0.2$)

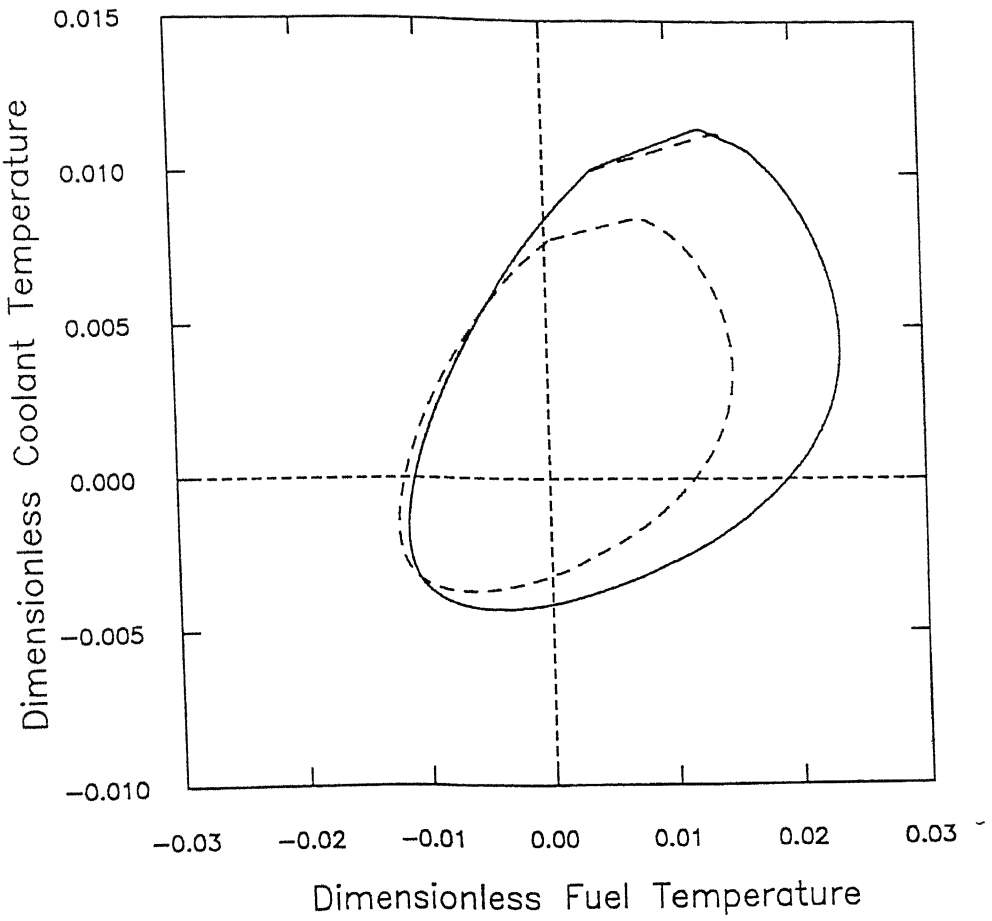

Figure 15 : Phase portrait of limit cycles in PHWR (220 MWe) for the core, core along with moderator, and core with moderator and Steam Generator on $\Im_f - \Im_c$ plane subsequent to Hopf bifurcation using one-group of delayed neutrons($\varepsilon = 0.2$)

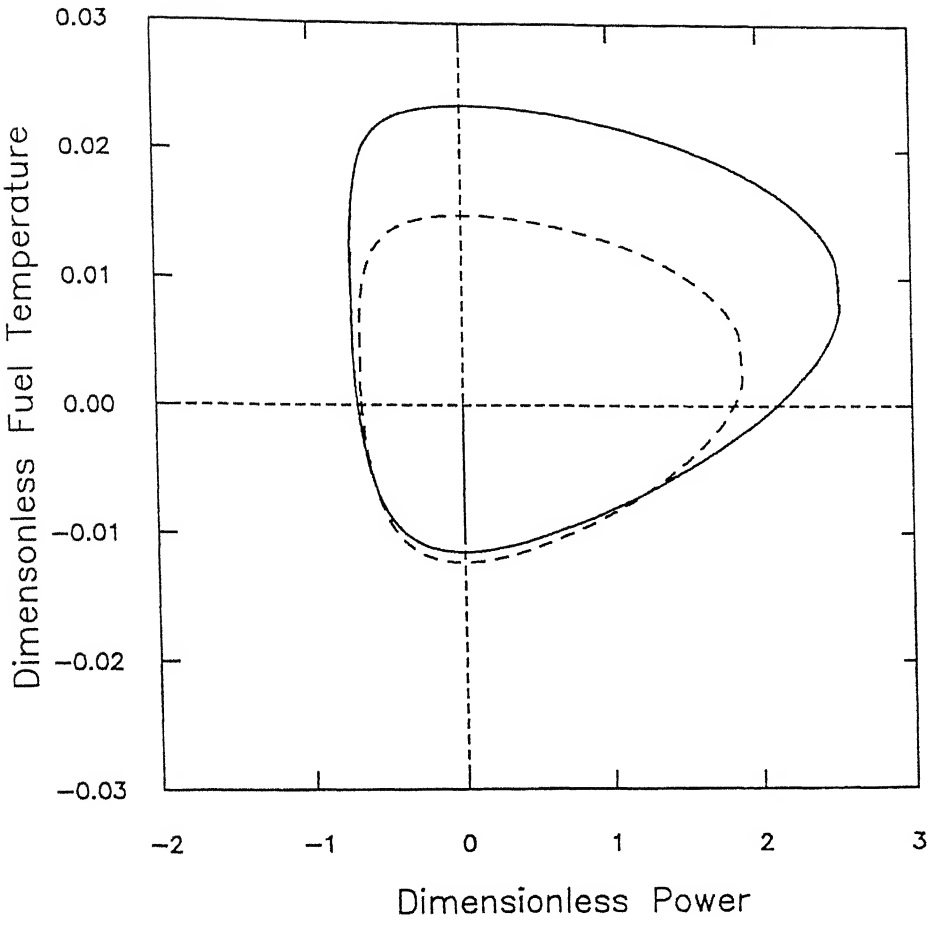

Figure 16 : Phase portrait of limit cycles in PHWR (220 MWe) for the core, core along with moderator, and core with moderator and Steam Generator on $\wp - \Im_f$ plane subsequent to Hopf bifurcation using one-group of delayed neutrons($\varepsilon = 0.2$)

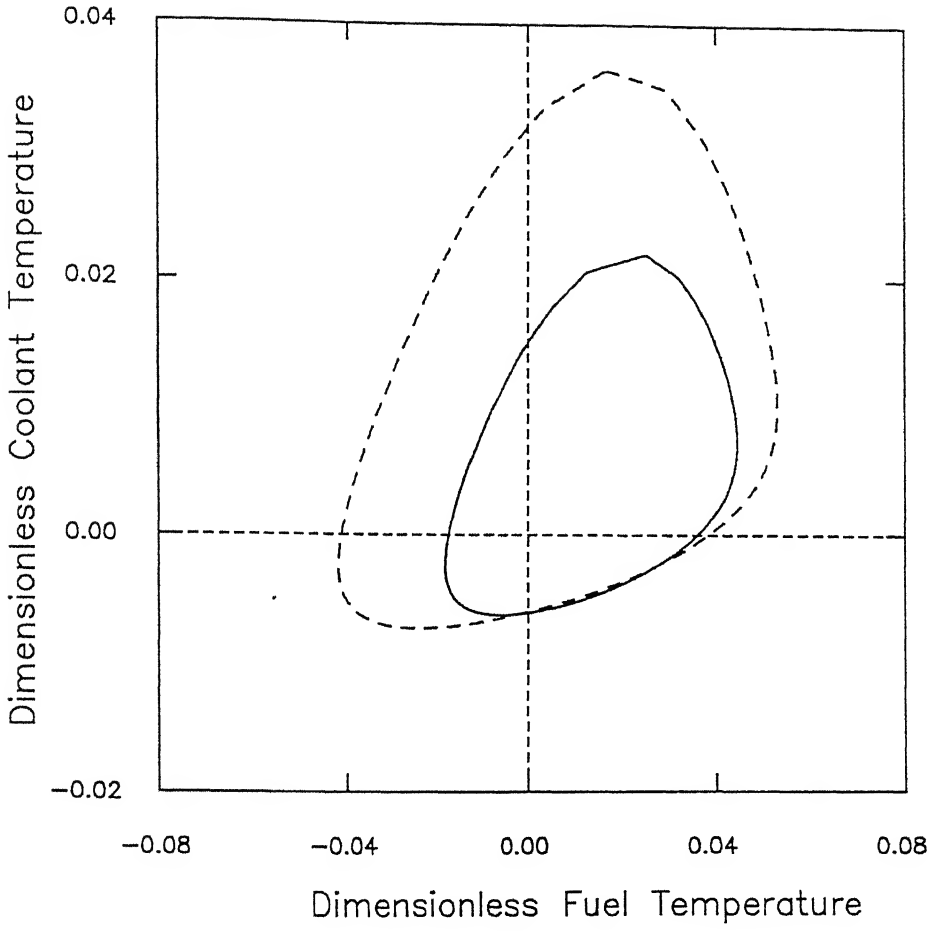

Figure 17 : Phase portrait of limit cycles in PHWR (500 MWe) for the core, core along with moderator, and core with moderator and Steam Generator on $\Im_f - \Im_c$ plane subsequent to Hopf bifurcation using one-group of delayed neutrons($\varepsilon = 0.2$)

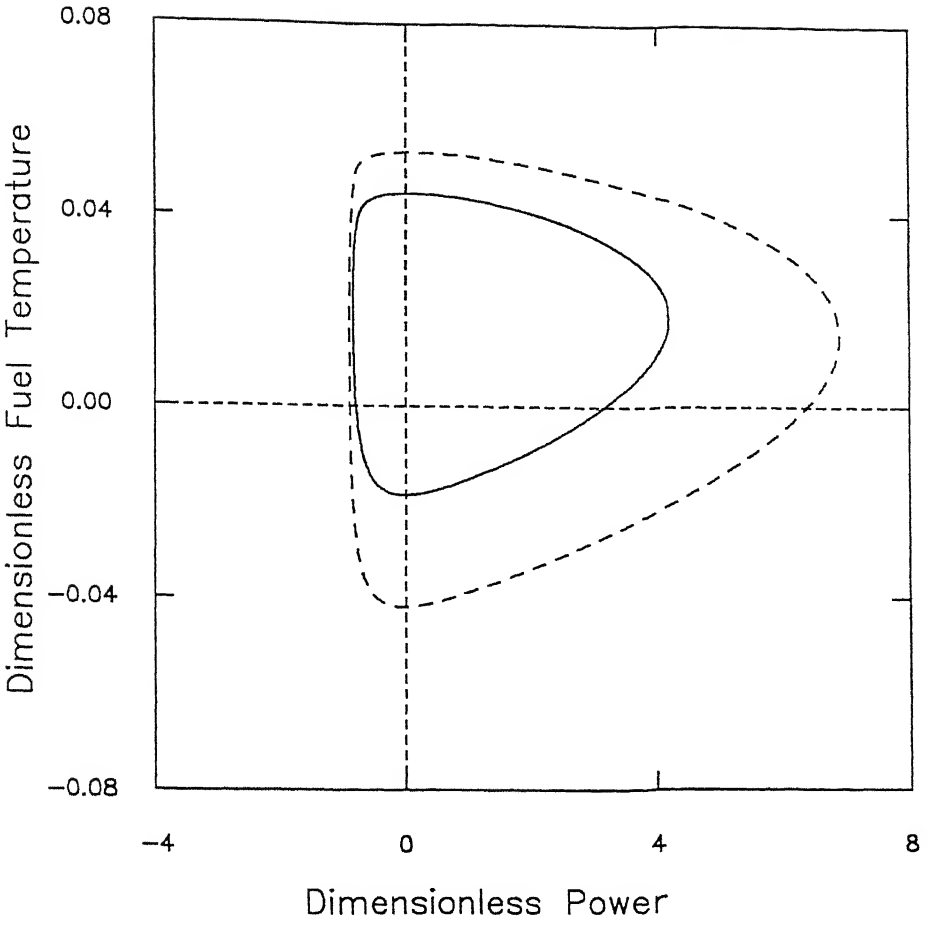

Figure 18 : Phase portrait of limit cycles in PHWR (500 MWe) for the core, core along with moderator, and core with moderator and Steam Generator on $\wp - \Im_f$ plane subsequent to Hopf bifurcation using one-group of delayed neutrons($\varepsilon = 0.2$)

References

Adebiyi, S. A. and Harms, A. A. (1989). On the topology of linear and nonlinear reactor kinetics. *Annals of Nuclear Energy*, **16**(11):605-609.

Adebiyi, S. A. and Harms, A. A. (1990). Behavioral geometrics of nonlinear reactor dynamics. *Journal of Nuclear Science and Technology*, **27**(5):416-430.

AERB (1997). Design safety guide on core reactivity control in PHWRs. Anenexure-I, *Atomic Energy Regulatory Board*, India.

Bagchi, T. P. (1994). Statistical investigation and robustness evaluation of PHWR fuel modelling and in-core performance. Phase 1 summary report, *Atomic Energy Regulatory Board*, India.

BARC (1987). Napp physics design manual. *Bhabha Atomic Research Centre*, India.

Bergdhal, B. G., *et al.* (1989). BWR stability investigation at forsmark 1. *Annals of Nuclear Energy*, **16**(10):509-520.

BHEL. Simulation studies of CANDU reactors in Indian power grids. Developement of model Volume 1, *Bharat Heavy Electricals Limited*, India.

Bruno, Alexander D. (1989). *Local Methods in Nonlinear Differential Equations.* Springer-Verlag

Chernick, Jack (1951). The dependence of reactor kinetics on temperature. Technical report. Brookhaven National Laboratory, Upton, N.Y., U.S.A.

Dorning, J. (1989). Is there a strange attractor in your reactor? *Transaction of the American Nuclear Society*, **60**:341-342.

Enginol, Turan B. (1985). On the asymptotic stability of nuclear reactors with arbitrary feedback. *Nuclear Science and Engineering,* **90**:231-235.

Glasstone, S. and Sesonske A. (1994). *Nuclear Reactor Engineering.* Chapman & Hall.

Guckenheimer, John and Holmes, Philip (1983). *Nonlinear Oscillations, Dynamical Systems. and Bifurcations of Vector Fields.* Springer-Verlag.

Hetrick, David L. (1965). A liapunov function in reactor dynamics. *Transactions of the American Nuclear Society*, **8**:477.

Hetrick, David L. (1971). *Dynamics of Nuclear Reactors.* University of Chicago Press.

Husseyin, Koncay (1986). *Multi Parmeter Stability Theory and Its Applications: Bifurcations, Catastrophies, ...* Clarendon Press.

Hsu, Chun (1968). A stability criterion for spatially dependent nonlinear reactor systems. *Transactions of the American Nuclear Society*, **11**:223.

Hsu, T. and Sha, W. T. (1969). Determination of stability domain of nonlinear reactor dynamics. *Transactions of the American Nuclear Society*, 12:295.

Kalra, M. S. and Sriram, K. (1998). Impact of nonlinear reactivity interactions and power excursions on safe operation of nuclear reactors. Consolidated report (Phase 1 and 2), *Atomic Energy Regulatory Board*, India.

Kastenberg, William E. (1968). On the stability of a reactor with arbitrary feedback. *Transactions of the American Nuclear Society*, 11:224.

Kubicek, M. and Marek, M. (1983). *Computational Methods in Bifurcation Theory and Dissipative Structures*. Springer-Verlag.

Lewins, J. (1978). *Nuclear Reactor Kinetics and Control*. Pergamon Press.

Manmohan, P. (1996). Nonlinear reactivity interactions in fission reactor dynamical systems. Ph.D. thesis, Indian Institute of Technology Kanpur.

NPCIL, (1992). Indian nuclear power programme with PHWRs. *Nuclear Power Corporation*, India.

Parker, T. S. and Chua, L. O. (1989). *Practical Numerical Algorithms for Chaotic Systems*. Sringer-Verlag.

Power Reactors (1983). Annual directory of data on the world's nuclear power reactors. *Supplement to Nuclear Engineering International, volume 28*.

Press, William H., et al. (1993). *Numerical Recipes in FORTRAN: The Art of Scientific Computing*. Cambridge University Press.

Rastogi, B. P. and Rustagi, R. S. (1976). Conceptual design aspects of heavy water reactors. *Bhabha Atomic Research Centre*, India.

Rizwan-uddin (1989). Space-independent Xenon oscillations revisited. *Transactions of the American Nuclear Society*, **60**:343-345.

Robinson, Lawrence Baylor (1954). Concept of stability of nuclear reactors. *Journal of Applied Physics*, **25**:516-518.

Robinson, Lawrence Baylor (1955). Effect of delayed fission neutrons on reactor kinetics. *Journal of Applied Physics*, **26:**52-56.

Ruelle, David (1989). *Chaotic Evolution and Strange Attractors*. Cambridge University Press.

Ward, Mary E. and Lee, John C. (1987a). Singular perturbation analysis of limit cycle behavior in nuclear-coupled density-wave oscillations. *Nuclear Science and Engineering*, **97**:190-202.

Ward, Mary E. and Lee, John C. (1987b). Singular perturbation analysis of relaxation oscillations in reactor systems. *Nuclear Science and Engineering*, **95**:47-59.

Wiggins, Stephen (1989). *Introduction to Nonlinear Dynamical Systems and Chaos*. Springer-Verlag.

World Nuclear Industry Handbook (1994). *Nuclear Engineering International.*

Yang, Chae Yong and Cho, Nam Zin (1992). Expansion methods for finding nonlinear stability domains of nuclear reactor models. *Anals of Nuclear Energy* , **19**(6):347-368.

Appendix A

Sample calculations of C_f , C_c and C_m

Estimation of C_f

$C_f = c_f m_f = 17.92$ MJK^{-1}, where

specific heat of fuel elements, $c_f = 0.32$ KJkgK^{-1}

fuel inventory, $m_f = 56 \times 10^3$ kg

$V_f = m_f / \rho_f = 56000 / 11000 = 5.09$ m^3, where V_f is volume of fuel elements, and

$\rho_f = 11000$ kgm^{-3} is the density of fuel material.

Estimation of C_c

fuel pellet diameter , d = 1.427 cm

clad thickness , t = 0.041 cm

$V_{clad} / V_{fuel} = 4t(d + t)/ d^2 = 0.118$

V (total volume of 306 pressure tubes/ coolant channels) = $(\pi / 4)\, d_i^2\, L \times 306$

$= (\pi / 4)\, (0.08255)^2 \times 6 \times 306$

$= 9.89$ m^3

where

inner diameter of pressure tube , $d_i = 0.08255$ m

active length of the pressure tube , L = 6 m

$V_f / V = 5.09 / 9.83 = 0.518$

$V_{clad} / V = (V_{clad} / V_{fuel}) \times (V_{fuel} / V) = 0.0613$

$V_{structure} / V = (V_{clad} / V) \times 1.2 = 0.0735$

(20% additional structure volume over and above the clad volume allowed in the pressure tubes.)

$(V_{fuel} + V_{structure}) / V_{total} = 0.5915$

$V_{coolant} / V = 0.4085 \cong 0.41$

$V_{coolant} = 0.41 \times 9.83 = 4.015\ m^3$

$m_{coolant} = V_{coolant} \times \rho_c = 3.21$ tonnes, where

density of coolant , $\rho_c = 800\ kg\ m^{-3}$

This value of $m_{coolant}$ has ben approximated to 3 tonnes.

$C_c = m_c c_c = 16.5\ MJK^{-1}$, where

specific heat of coolant , $c_c = 5.5\ KJkg\ K^{-1}$

Estimation of C_m

$C_m = m_m c_m$, where

m_m is mass of moderator in the calandria, and

specific heat of the moderator , $c_m = 4.2\ kJK^{-1}$.

m_m has been estimated as follows:

Calandria volume = $(\pi / 4) D^2 L \cong 100\ m^3$,

where D and L are the diameter and active length of the calandria.

For the present calculation D ≅ 5m , L ≅ 5m.

Volume displaced by the coolant channels / pressure tubes = $(\pi / 4)\, d_o^2\, L \times 306$

$= (\pi / 4)\, (0.12)^2 \times 5 \times 306$

$= 17.3\ m^3$

where

outer diameter of the pressure tube , $d_o \cong 0.0012$ cm

$V_{moderator} = (100.0 - 17.3)\ m^3 = 82.7\ m^3$

$m_m = V_{moderator} \times \rho_m = 80$ tonnes, where

density of the moderator, $\rho_m = 1100\ kg\ m^{-3}$

Thus approximated 60 % of the total moderator calculation inventory of 137 tonnes (NPCIL, 1992) is in the calandria. We have made a similar assumption for the other reactors to calculate the mass of the moderator in the calandria.